

2014

Wageningen UR

Dekker, Iris



# [NO<sub>x</sub> CONCENTRATIONS AND EXPOSURE IN AMSTERDAM AND OVER EUROPE]

A study based on joint high resolution WRF modelling and observations



## Abstract

Simulations with the Weather Research and Forecast model were done, using its chemistry core (WRF-chem) for simulating tracer transport. Over Amsterdam a model resolution  $1 \times 1 \text{ km}^2$  was used. Nitrogen oxides ( $\text{NO}_x$ ) emissions and  $\text{O}_3$  background concentrations over Europe were implemented;  $\text{NO}_x$  was partitioned into nitrogen oxide (NO) and nitrogen dioxide ( $\text{NO}_2$ ). A simple chemistry scheme was applied. Monitoring network measurements of NO,  $\text{NO}_2$  and  $\text{O}_3$  are used to validate the model for Amsterdam; OMI-satellite observations were used for evaluation of concentrations over Europe and the Netherlands. The objectives were evaluating WRF's representation of  $\text{NO}_x$  on city and European scale with the relative simple input and assessing bicycle commuter exposure levels in Amsterdam at different meteorological conditions and departure times. The city scale performance of WRF was varying ( $R^2$ : 0.007 to 0.931) and best for city background stations. Of the two days compared to satellite, for one the model and satellite were comparable, but the  $\text{NO}_2$  column values of the Ruhr-area plume were underestimated and shifted to the North. For the other day large underestimations were found, this could have been partly due to too slow NO to  $\text{NO}_2$  conversion. With the model, the choice of route to the city centre and the departure time were found important in determining the exposure. Differences of more than 100% were found between different times of cycling. Routes downwind of the city have higher exposure; winds from the south east of Amsterdam bring high concentrations. Acting according to this knowledge could improve the health of Amsterdam's cycle commuters.

**Keywords:**  $\text{NO}_2$ ,  $\text{NO}_x$ , air quality modelling, exposure, departure time, meteorology, city scale, high resolution, Weather Research and Forecast model, WRF, WRF-chem, satellite comparison, Amsterdam, Netherlands.

## Acknowledgements

I would like to thank my supervisors Michiel van der Molen and Bert van Hove for supporting me in this thesis by giving a critical view to my work, providing relevant literature and sharing their knowledge. Michiel van der Molen as well as Denica Bozhinova have been of much help in using Python and WRF and making WRF scripts. I would like to thank Folkert Boersma for his help in processing the OMI satellite data. Further, we would like to acknowledge TNO for using the MACC emission database, GGD Amsterdam for providing measurement data on pollutants and temperature. We acknowledge as well the free use of tropospheric NO<sub>2</sub> column data from the OMI sensor from [www.temis.nl](http://www.temis.nl).



Source front page picture: <http://www.abvvjongeren.be/art.cfm?pid=27609>

# Table of Contents

Abstract .....	ii
Acknowledgements .....	iii
Summary .....	v
1. Introduction .....	1
2. Background information.....	3
2.1 Nitrogen oxides and air pollution in general .....	3
2.2 Modelling urban air quality .....	4
3. Materials and Methods.....	6
3.1 Data .....	6
3.1.1 Weather data .....	6
3.1.2 Emission data .....	6
3.1.3 Validation data .....	6
3.1.4 Bicycle-traffic intensity data.....	8
3.2 WRF and WRF-chem .....	8
3.2.1 Domains and resolution.....	8
3.2.2 NO <sub>x</sub> partitioning .....	9
3.2.3 NO <sub>x</sub> deposition .....	9
3.2.4 NO <sub>x</sub> chemistry .....	9
3.2.5 Ozone boundary conditions.....	10
3.3 Data preparation for WRF.....	10
3.3.1 providing chemistry input .....	11
3.3.2 Implementing more refined 1x1 km <sup>2</sup> emissions .....	11
3.4 Commuters' Exposure.....	12
3.5 Satellite comparison .....	13
3.6 Implementation of the different runs .....	13
4. Results .....	15
4.1 Validation of the model for temperature and NO <sub>2</sub> .....	15
4.2 Sensitivity analysis.....	18
4.3 Spatial patterns .....	19
4.4 Daily patterns in NO <sub>x</sub> for different weather situations.....	19
4.5 Commuters' exposure.....	22
4.6 Satellite comparison .....	24
5. Discussion.....	26
5.1 Validation.....	26
5.2 Temporal and spatial patterns.....	29
5.3 Commuters' exposure .....	31
6. Conclusions.....	34
7. Recommendations .....	35
References.....	36
Appendix .....	39

## Summary

In this study, we modelled the temporal and spatial variability of nitrogen oxide species and ozone in Amsterdam. This is done at the high resolution of  $1 \times 1 \text{ km}^2$  in the Weather Research and Forecast model (WRF) and its chemistry core (WRF-chem). The objectives of this study were assessing the variability in commuters' exposure under different meteorological conditions and departure times and evaluating WRF's representation of  $\text{NO}_x$  on city and on European scale with relative simple chemistry input. The model was validated with data obtained from the air quality monitoring network in Amsterdam and with European satellite data.

Large-scale meteorological input for the WRF model was obtained from NCEP reanalysis data. European  $\text{NO}_x$  emissions from the TNO-MACC database with a resolution  $1/8^\circ \text{lon} \times 1/16^\circ \text{lat}$ , were implemented in the model. Emissions over Amsterdam were specified at  $1 \text{ km} \times 1 \text{ km}$  resolution. In a WRF subroutine,  $\text{NO}_x$  was partitioned into  $\text{NO}$  and  $\text{NO}_2$  and a simple deposition and chemistry scheme were applied. Ozone was implemented by setting ozone boundary conditions and input ozone concentrations on 30 ppb and above 3 km height on 35 ppb. One outer domain over Europe and two nested domains over the Netherlands and Amsterdam were used. The resolutions of the domains were respectively:  $8 \times 8 \text{ km}^2$ ,  $4 \times 4 \text{ km}^2$  and  $1 \times 1 \text{ km}^2$ . For investigating commuters' exposure to  $\text{NO}_2$  two main and two alternative routes were chosen, the routes traverse the city from east to west and from south to north. Measurements of  $\text{NO}_2$ ,  $\text{NO}$ , ozone and temperature done by the GGD Amsterdam on different locations in the city were used to validate the model for Amsterdam. OMI-satellite observations were used to validate the model on a larger scale. Runs were done for six periods in 2013: March 25-28, April 19-22, April 22-25, July 6-9, July 10-13 and July 22-25. These periods were chosen for their differences in temperature, wind direction and sun hours per day. The commuters exposure was investigated for March 25, April 23, July 10 and July 22. On these days the  $R^2$  during rush hours for  $\text{NO}_2$  were found highest.

WRF represented the daily temperature cycle very well, but underestimated the absolute values by around two degrees. In general, the model results for  $\text{NO}_2$  and  $\text{NO}$  were found to be moderately to highly correlated with the observations of the background stations Vondelpark, Sportpark Oostmeerpark and Oude Schans Centrum ( $R^2$  up to 0.84). The ability of the model to capture the  $\text{NO}_2$  concentrations differed, however, by day. For some modelled periods the performance of the model was worse, especially for the cold period of 25-27 March, where concentrations were highly underestimated and for the hot days 21-23 July where the daily pattern was modelled wrong, possibly due to the stable smog conditions which were present, but not modelled by WRF. For the urban background stations in Amsterdam in 2013 a yearly average  $\text{NO}_2$  concentration of  $25.9 \mu\text{g}/\text{m}^3$  was found. The average concentration over 2013 for traffic station Stadhouderskade was  $39.8 \mu\text{g}/\text{m}^3$ . Two days were suitable for satellite comparison: July 8 and March 27. For the former the model and satellite data were comparable: over a large part of West-Europe, the concentrations were in the right order of magnitude and general plumes and high concentration areas are the same. However the modelled plume from the Ruhr-area had lower concentrations than the concentrations found by the satellite and the modelled plume was somewhat more east-west orientated and extended longer than the satellite plume. For March 27 less similarities and large underestimations were found, this could have been partly due to a too slow  $\text{NO}$  to  $\text{NO}_2$  conversion.

The differences found in exposure on different departure times and with different choice of routes, were found large (more than 100%). For March 25 and April 23, the lowest exposure of the morning was found for a departure at 7 am LT, before the start of the morning rush hour. For the two summer days July 10 and July 22, the best time of departure was at 8 am LT and 10 am LT, the optimum between rapid boundary layer growth, and thus vertical mixing on the one side and on the other side the accumulation of emissions during the morning. In the afternoon, least exposure was found for the departure at 4 pm LT – and 5 pm LT for July 22 – when the boundary layer height was maximal. Winds over the city and from the south-east of Amsterdam were found to bring higher polluted air; the choice of a route upwind of the source or downwind of a low emission area like the IJmeer, could give lower exposure values; differences in exposure by choice of route were found to be up to 60%.

The most important conclusion is that the choice of route to the city centre, the departure time and meteorology are important for determining the exposure value. Differences of more than 100% were found between different times of cycling. The wind direction influences the cleanest cycle route, higher exposure have been found with winds coming from upwind sources like the city centre or the south-east

of Amsterdam. The development of the mixed layer is important in determining the extent to which  $\text{NO}_2$  is accumulated or spread in the vertical.

# 1. Introduction

Air quality is a critical issue all around the world. Many megacities, especially in South-eastern Asia, are dealing with high concentrations of pollutants (Chan and Yao, 2008; Mönkkönen et al., 2005). The high level of air pollutants threaten the health of those citizens. However, in many cities in Europe as well annual average NO<sub>2</sub> concentrations are still above the guidelines of the World Health Organisation (WHO, 2011). In Amsterdam the GGD measured in 2012 at 77% of the street stations exceedances of the WHO guidelines and the European limits to NO<sub>2</sub> (RIVM, 2013b).

Air pollution reached the Dutch newspapers headlines several times last months. In e.g., NRC (Willems, 2013) and Volkskrant (Heijne, 2013), the headlines stated that that the quality of the air in Dutch cities "remains poor" and EU norms are exceeded several times in cities of the Netherlands. In Rotterdam and Amsterdam the increase of the speed limits were to be reconsidered as a result of the high nitrogen dioxide measurements along roads (Deira, 2014) and on February 25 it was decided that the speed limit must be brought back to 80 km/hour by the end of March (ANP, 2014).

As the negative impact of air pollution on human health has become clear e.g. (e.g. (Bernstein et al., 2004; Pope III and Dockery, 2006)), air quality monitoring network are established and extended for several decades. The measurements, however, do only give an indication of the air quality in the close surroundings of the measurement points. To be able to get a good overview of pollutant concentrations at places where people spend their time or where people live, or to be able to look at average pollutant concentrations along roads, a model is needed to provide a spatial pattern in the pollutant concentrations under different circumstances. As pollutant concentrations are dependent on numerous different factors, e.g., emissions, building structure, meteorology, making a model that represents the concentrations on city scale is quite an advantage and no perfect model has been developed yet.

Work has been done on modelling the nitrogen oxide and ozone chemistry on city scale for example by Berkowicz (Berkowicz, 2000b) who developed the Urban Background Dispersion Model, as well as the Operational Street Pollution Model (OSPM; Berkowicz, 2000a)). In the Netherlands, the CAR-II model (Calculation of Air pollution from Road traffic) was developed (Den Boeft et al., 1996). These models all include a very simple chemistry scheme and only meteorology data on incoming radiation and wind speed and direction. However, these models need very specific input on buildings, roads and emissions in a city. The OSPM has been tested in several cities in the Northern Hemisphere and gives reasonable results for NO<sub>x</sub> and O<sub>3</sub> most of the time (Kakosimos et al., 2010). The models, however, are not coupled to numerical weather prediction models. This makes results on hourly basis, which are very dependent on the meteorological conditions less accurate than longer period averages (Kakosimos et al., 2010). Besides, the OSPM studies are usually performed for only one or a few streets, and lack the overview of city wide concentrations (Kakosimos et al., 2010). Furthermore, studies have been done with a fully coupled chemistry Weather Research and Forecast (WRF-chem) model, modelling city scale NO, NO<sub>2</sub> and ozone. Elshazly et al. (2012) performed a study over Cairo. They were not able to model reasonable NO<sub>x</sub> values, R<sup>2</sup> of 0.007 and correlation coefficients of -0.08 were found. However, the emissions used were on a scale of 1°lat x 1°lon and model resolutions were 27km x 27km. Zhang et al. (2009) performed a higher resolution study of 3 km x 3 km over for Mexico city. They compared the model results with measurements over 12 ground stations. For NO and NO<sub>2</sub> correlation coefficients found were overall 0.43 and 0.45 for NO and NO<sub>2</sub> respectively. Tie et al. (2010) compared the performance of WRF-chem for 3, 6, 12 and 24 km resolution and showed high improvement in predicting NO<sub>x</sub> and ozone with higher resolution. This is promising for our study, where NO<sub>x</sub> concentrations will be modelled on an even higher resolution of 1x1 km<sup>2</sup>.

A WRF-chem study has not been done for the Netherlands yet. This MSc thesis project will be the first assessment on modelling nitrogen oxide species and ozone in Amsterdam, on a high resolution of 1x1 km<sup>2</sup> and with a simple chemistry scheme included. The influence of meteorological conditions on urban air pollutant concentrations and commuters' exposure are examined. The study is performed for Amsterdam, the capital city of the Netherlands.

Focus is on nitrogen oxides (NO and NO<sub>2</sub> - which together are called NO<sub>x</sub>) and ozone (O<sub>3</sub>), an important player in the reaction with NO<sub>x</sub>. Together they are the main constituents of photochemical smog. The objective of this study is to assess the levels of these pollutants to which citizens are exposed at different weather conditions.

The research questions are:

- How well does the model represent pollutant levels and weather conditions in Amsterdam?
- How do NO<sub>2</sub> concentrations compare to satellite observations over the Netherlands and Western Europe?
- What are the concentrations of pollutants found in Amsterdam?
- Are there differences in the amount of pollution on the different main (bicycle) routes to the city centre?
  - Is the 'healthiest' route to (cycle to) the city centre dependent on the weather type?
  - What is the influence of departure time on exposure?

Observations as well as results of model simulations will be used in this assessment. The observations will be used to validate the results of the model simulations. Subsequently, model simulations are done to examine to which extent the air of in Amsterdam is polluted under different weather circumstances. Particular emphasized will be the air quality around the most intense used bicycle lanes for investigating which level of pollution bicycle commuters are exposed to. Modelling the pollution distribution in Amsterdam on the relative small scale of 1x1 km<sup>2</sup>, may contribute to the awareness and health of Amsterdam's citizens and commuters.

Besides looking at the small scale, also the larger scale will be taken into account: a comparison of the model with satellite observations over the Netherlands and Western Europe will be done. The objective is to investigate whether the large scale nitrogen dioxide patterns and thus the advection terms are represented well.

## 2. Background information

### 2.1 Nitrogen oxides and air pollution in general

Air pollution consist of a mixture of small particles and chemical species which can form a threat for the health of humans, plants (crop growth) and animals. The degree of pollution not only depends on the amount of pollutants that is emitted but also on the weather situation. A high stability of the air with low wind speeds and little incoming radiation e.g. can lead to a build-up of pollutant concentrations, whereas high wind speeds and buoyance result in well mixed air with low pollutant concentrations. The two most threatening pollutants for human health are surface ozone and particulate matter (Jacob and Winner, 2009). However, the focus of this paper will be on nitrogen oxide species, which are mainly traffic related pollutants.

For nitrogen dioxide (NO<sub>2</sub>) the European commission has set legislative limits. On April, 7 2009, the European Commission (EC) respited the Netherlands to meet the limits – other EU countries had already to cope with the new limits in 2010. For NO<sub>2</sub> the legislative limits are yearly average values of 40 µg/m<sup>3</sup> from January 1<sup>st</sup> 2015 on. This is according to the WHO guidelines. Until that date, the limit is 60 µg/m<sup>3</sup> for the yearly average concentration (EC, 2013; GGD, 2012). For ozone the target value – so no legislation - is less than 120 µg/m<sup>3</sup> averaged over 8 hours (EC, 2013).

Measurements of the National Air Quality Network of the Netherlands (LML) of RIVM, GGD-Amsterdam<sup>1</sup> and DCMR<sup>2</sup> showed that the concentrations of PM<sub>10</sub> and NO<sub>2</sub> follow a long-term downward trend. However, the yearly average NO<sub>2</sub> concentration for traffic stations in 2012 was 38 µg/m<sup>3</sup> and for Amsterdam this was even 45 µg/m<sup>3</sup>. The average background concentration of 2010 was 18 µg/m<sup>3</sup>, city background stations in Amsterdam measured on average 30 µg/m<sup>3</sup> in 2012. While PM<sub>10</sub> is not exceeding on any location the EU air quality norms last years, for NO<sub>2</sub> in 2012 half of the traffic stations (in Amsterdam even 77%) was exceeding the 2015 limits, and is very likely that the limits are still not met in 2015 (GGD, 2012; RIVM, 2012, 2013b). In addition, the concentration nitrogen dioxides (NO<sub>2</sub>) has decreased less than the measured concentration nitrogen oxides (NO<sub>x</sub>), which is probably caused by the increase in the fraction NO<sub>2</sub> emitted by traffic (RIVM, 2013b).

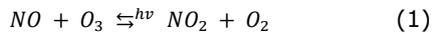
NO<sub>x</sub> is part of the mixture of traffic-related air pollution and is often used as an indicator for the total complex mixture of gases originating mainly from traffic (RIVM, 2013a). This means that NO<sub>x</sub> in the air most of the time goes along with harmful particulate matter and black smoke from vehicles (Knol, 2013). An advantage of using NO<sub>x</sub>-species is that they are relative easy to measure. NO<sub>2</sub> at the concentrations which are measured on average in the Netherlands, are not harmful for the public health according to the RIVM (RIVM, 2013a). Though, NO<sub>2</sub> is reactive and can cause problems with eyes and inflammation of the lungs when exposed for short time to high concentrations. The WHO short-term exposure guideline is a maximum concentration 200 µg/m<sup>3</sup> as annual mean (WHO, 2011). Besides, long-term exposure to lower concentrations has in different studies been associated with higher mortality rates. In the review study of Hoek et al. (2013), 15 previous studies on long-term health effects of NO<sub>2</sub> have been pooled, leading to the conclusion that all-cause mortality was significantly associated with NO<sub>2</sub>: per 10 µg/m<sup>3</sup> the mortality was estimated 5% (with a 95% confidence interval of 3%-8%). This has been based as well on a Dutch study (Beelen et al., 2008), in which for a NO<sub>2</sub> increase of 30 µg/m<sup>3</sup> relative risks on mortality of 1.08 (95% confidence interval 1.00-1.16) was associated with a natural cause death and 1.37 (95% confidence interval 1.00-1.87) with respiratory diseases. This is higher than the relative risk found on mortality associated with a PM<sub>2.5</sub> increase of 10µg/m<sup>3</sup> – these were 1.06 (95% CI 0.97-1.16) and 1.07 (95% CI 0.75-1.52) for natural cause and respiratory respectively. NO<sub>2</sub> is probably not the cause of the health problems in this studies, but is nonetheless associated to mortality as NO<sub>2</sub> is an indicator of traffic-related air pollution as mentioned before. NO<sub>2</sub> has thus a mortality indicator role, it is an indicator for traffic and industry related air pollution and it plays an important role in the formation of smog by the reaction with ozone. Besides, NO<sub>2</sub> is a precursor of nitrates which contribute to the amount of particulate matter in the atmosphere. Taking all these factors together, it is important to be aware of the NO<sub>2</sub> levels in the atmosphere. In addition, PM consists of particles of different primary and secondary sources, including sea salt and dust, while NO<sub>2</sub> is a molecule emitted solely by burning processes.

---

<sup>1</sup> the health institute of Amsterdam, also for environmental issues

<sup>2</sup> the environmental protection agency of Rotterdam

NO<sub>x</sub> is emitted at high temperature (fossil fuel) burning processes. Traffic and industry are the main sources. NO<sub>x</sub> is mainly emitted as NO by motor vehicles; only a small part is emitted as NO<sub>2</sub>. NO reacts with ozone to form the somewhat more toxic NO<sub>2</sub>. The reverse of this reaction takes place only under sunlight conditions when photo dissociation of NO<sub>2</sub> leads to partial reproduction of NO and O<sub>3</sub>. In Equation 1, the forward and backward reactions are shown (Berkowicz, 2000a, b; Collins et al., 1997).



The rate constant of the forward reaction as well as the photo dissociation rate of the backward reaction are described in Section 3.3.2 under NO<sub>x</sub> chemistry.

Tropospheric, or ground level ozone is a secondary pollutant, i.e. it is not directly emitted but formed in chemical reactions. For ozone these reactions are driven by sunlight, involving CO, VOCs including CH<sub>4</sub>, and NO<sub>x</sub> (Fowler et al., 2008). Ozone is toxic to humans and vegetation, but is usually a regional rather than urban pollution problem because of the rapid reaction with NO, which is abundant in most cities. The largest ozone pollution problems are for that reason usually found downwind of cities (Jacob, 1999). However, during stagnating and high temperatures, ozone can become a problem as well in cities. The formation of ozone is a chain reaction mechanism, which is initiated by the production of HO<sub>x</sub> (HO<sub>x</sub> ≡ H + OH + HO<sub>2</sub>). Other species involved in the reactions forming ozone are as named before CO, and NO<sub>x</sub> (according to the reaction in Equation 1) and hydrocarbons (RH; R is an organic group), OH, RO<sub>2</sub> and the carbonyl compound R'CHO. Important mechanisms in the tropospheric ozone - nitrogen oxide chemistry, such as the NO-NO<sub>2</sub> cycle, and ozone destruction by OH, can be found back in Figure 1.

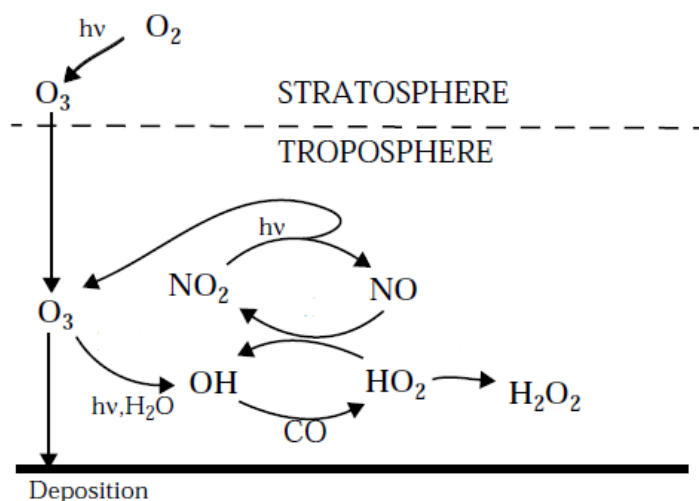


Figure 1 Adapted from (Jacob, 1999): Mechanism for O<sub>3</sub>-HO<sub>x</sub>-NO<sub>x</sub>-CO chemistry in the troposphere

## 2.2 Modelling urban air quality

The advantage of modelling is that you can get an impression of the temporal and spatial variability of air pollutants. In addition, you get an impression of the vertical profiles of air pollutants in the urban boundary layer. The use of labelled emissions, as was done in our research, makes it possible to determine the sources of NO<sub>x</sub> on different locations and times.

Using the Weather Research and Forecast model (WRF) and its chemistry core for modelling NO<sub>x</sub> over Amsterdam and Europe has advantages over the use of models which use only a limited meteorological input. The meteorological conditions are very important in determining pollutant concentrations. In WRF it is possible to use a large amount of meteorological variables for determining the spreading of tracers. This is most importantly enabled by WRF's higher order numerics, time-split integration, higher order advection schemes in both horizontal and vertical directions, the ability to represent turbulence and use of microphysics and surface physics schemes (Grell et al., 2005; Skamarock et al., 2008). Besides, in WRF it is possible to run with nested domains, where the larger domain provides the boundary conditions for the smaller domain, making it very suitable for use on a high resolution of up to about one kilometre combined with advection of pollutants, defining background concentrations, from larger areas with a lower resolution. In short, in WRF-chem horizontal transport of pollutants is combined with vertical

mixing, where the height and stability of the boundary layer is taken into account. It additionally is possible to take light-dependent reactions into account as radiation terms are included in the model as well.

In the commonly used street level dispersion models like OSPM (Berkowicz, 2000a; Kakosimos et al., 2010) and CAR (Den Boeft et al., 1996), very specific input data is needed: heights of buildings along streets, as well as the width and orientation of the street, data on time variation in traffic and on traffic type (e.g. light or heavy), emission data for each type of traffic, hourly meteorological data on wind speed, wind direction, radiation and temperature, hourly background concentration of pollutants, the urban background concentration of  $\text{NO}_2$ ,  $\text{NO}_x$  and  $\text{O}_3$  and percentage of emitted  $\text{NO}_2$  (Nguyen and Wesseling, 2009). In our study we do not implement all these variables but only make use of calculated meteorology on basis of 6-hourly input, of standardized hourly  $\text{NO}_x$  emissions and of ozone background concentrations. This makes it suitable to use for any place in Europe, but WRF is less suitable for use on street scale: it will possibly give biases in streets with high emissions or with high buildings where local emissions determine for a very large part the concentrations.

## 3. Materials and Methods

### 3.1 Data

For running WRF different sources of weather input data were needed as initial and boundary conditions. Local pollutant measurements were used to validate the WRF model for NO<sub>x</sub> in the city of Amsterdam. For modelling NO<sub>x</sub> and ozone chemistry with WRF-chem, pollutant emission data were needed as well. All used data are described below.

#### 3.1.1 Weather data

The initial and boundary conditions for WRF were provided by 6-hourly reanalysis data from the National Centers for Environmental Prediction (NCEP reanalysis). The used dataset was the FNL Operational Model Global Tropospheric Analyses, continuing from July 1999 (Service/NOAA/U.S., 2000, updated daily). Data for 2013 was extracted.

#### 3.1.2 Emission data

Data on NO<sub>x</sub> emission were provided by the TNO-MACC (Monitoring Atmospheric Composition and Climate) emission database (Kuenen et al., 2011). The resolution of the emissions is 1/8° lon x 1/16° lat (about 8km x 8km) and is given per year. The emissions were expressed as kilograms NO<sub>x</sub> in NO<sub>2</sub> equivalents per year and are recorded from all countries of Europe. The data is divided in 15 different categories and for this research combined to nine categories (Table 1). Factors which differ between month of the year, day of the week and hour of the day for every category were provided as well to specify the emissions on hourly basis. These factors can be found back in Appendix 1 of the TNO report (van der Gon et al., 2011).

**Table 1 Different categories of the NO<sub>x</sub> emissions dataset by TNO-MACC and way of use in this research**

Category	Description	Used as: (NO <sub>x</sub> -, NO-, NO <sub>2</sub> - )
100	Power generation	100
200	Residential, commercial and other combustion	200
300	Industrial combustion	300
400	Industrial processes	Indu <sup>2</sup>
500	Extraction, distribution of fossil fuels	Indu <sup>2</sup>
600	Solvent use	--- <sup>1</sup>
701	Road transport gasoline	701
702	Road transport diesel	702
703	Road transport lpg	703
704	Road transport evaporation	--- <sup>1</sup>
705	Road transport brakewear	--- <sup>1</sup>
800	Other mobile sources	800
900	Waste treatment and disposal	Indu <sup>2</sup>
1000	Agriculture	1000

<sup>1</sup>NO<sub>x</sub> is not emitted as a result of solvent use, evaporation or break wear, so these categories are excluded.

<sup>2</sup>On the basis of a quantification of the emissions, the emission of NO<sub>x</sub> from categories 400, 500 and 900 were found low and are therefore combined to one category: Indu (industrial processes, fossil fuel extraction and distribution and waste treatment and disposal).

#### 3.1.3 Validation data

For the validation of the model, measured NO, NO<sub>2</sub> and O<sub>3</sub> data and data on temperature were obtained from GGD Amsterdam, they provided data of background as well as of traffic locations. In Figure 2 all measurement stations in (the surroundings of) Amsterdam are depicted.

GGD Amsterdam has 11 measurement stations in Amsterdam of which:

- 5 are traffic stations (Haarlemmerweg (A), Van Diemenstraat (B), Stadhouderskade (C), Einsteinweg (D), Jan van Galenstraat(E));
- 6 are urban background stations (Vondelpark (station Overtoom (F)), Westerpark (G), Sportpark Ookmeer (H), Nieuwendammerdijk (I), Kantershof (J) en Oude Schans (K)).

Besides, GGD Amsterdam has 4 measurement stations located in the close surroundings of Amsterdam:

- 1 is a traffic station (Hoogtij (L));

- 3 are urban background stations (Hemkade (M), Spaarnwoude (N), Zaandam(O)).

The LML-RIVM has 1 extra station located in Amsterdam:

- Amsterdam A10-west, which is a traffic station (P).

All stations have hourly data available, in micrograms per square meter, rounded to integers, and available from about January 2001 till January 2014 (only validated data available). In Table 2 can be found which of the pollutants of importance for our research are measured on which locations.

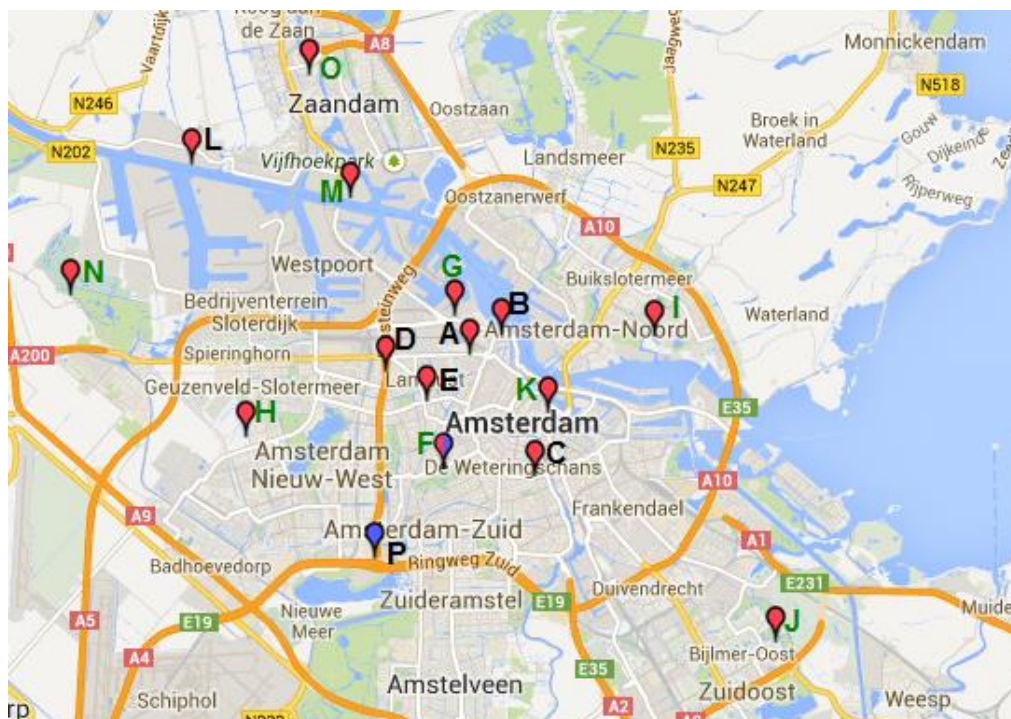


Figure 2 Locations of the GGD (Red arrows) and RIVM-LML (Blue arrows) measurement stations. The letters are described in the text. Green letters are urban background stations; black letters are traffic stations.

Table 2 Description of measured pollutants (nitrogen monoxide (NO), nitrogen dioxide (NO<sub>2</sub>) and ozone (O<sub>3</sub>)) on the 16 GGD and LML-RIVM stations. "Yes" means the particular pollutant concentration is measured.

Station	Station name	NO	NO <sub>2</sub>	O <sub>3</sub>
A	Haarlemmerweg	yes	yes	no
B	Van Diemenstraat	yes	yes	yes
C	Stadhouderskade	yes	yes	no
D	Einsteinweg	yes	yes	no
E	Jan van Galenstraat	yes	yes	no
F	Vondelpark	yes	yes	yes
G	Westerpark	no	no	no
H	Sportpark Ookmeer	yes	yes	no
I	Nieuwendammerdijk	yes	yes	yes
J	Kantershof	yes	yes	no
K	Oude Schans	yes	yes	no
L	Hoogtij	yes	yes	no
M	Hemkade	yes	yes	no
N	Spaarnwoude	yes	yes	no
O	Zaandam	yes	yes	yes
P	A10-west	no	no	no

### 3.1.4 Bicycle-traffic intensity data

Amsterdam is the largest city in the Netherlands with a population of 802,445<sup>3</sup> people (CBS, 2013). There are about 881,000 bicycles in Amsterdam (Fietsberaad, 2012) and the bicycle use has been growing the past 20 years with over 40 percent from 340,000 to 490,000 bicycle rides daily (DIVV, 2012b). In 2008 the transport in, towards and from the centre of Amsterdam was divided as follows: 30% of the movements was by bike, 34% by car and 16% by public transport (DIVV, 2012a). So, it can be said that cyclists form an important group of traffic in Amsterdam. And, as cyclist cycle directly in the open air and inhale usually more pollutants as result of their higher minute ventilation, it is especially important for this group to know the air pollution level in Amsterdam.

Information on the bike traffic intensity on roads were obtained from maps of 'Dienst Infrastructuur Verkeer en Vervoer Amsterdam' (DIVV, 2012b).

## 3.2 WRF and WRF-chem

For the simulations, the Weather Research and Forecasting (WRF) model, version 3.2.1 is used. The research core used is Advanced Research WRF, which is a non-hydrostatic meso-scale model developed at the National Centers for Environmental Prediction (NCEP). It has several choices for physical parameterizations, which allows the model to be applicable on many different scales (Grell et al., 2005). A build-in application is WRF-chem. WRF-chem is an online model, which means that it is consistent with all conservative transport done by the meteorology model. WRF-chem is used in modelling chemical processes and is able to take into account: dry deposition; aqueous phase chemistry coupled to microphysics; biogenic emissions; anthropogenic emissions; gas-phase chemical reaction calculations; photolysis schemes; aerosols and tracer transport.

In this research, only the model's tracer transport function was used, not the programmed chemistry of WRF. The chemistry was implemented by making subroutines with the (photo-chemical) reactions and running these in WRF (section 3.2.2).

In WRF different boundary layer schemes and surface layer schemes can be used. In this research the Mellor–Yamada–Nakanishi–Niino (MYNN) 2.5 order local closure Turbulence Kinetic Energy (TKE) scheme was used as boundary layer scheme (Janjić, 2002); for the surface layer, the MYNN surface layer option is used. MYNN is a local mixing scheme, i.e. there is only exchange between two adjacent layers (Stensrud, 2007), with a 2.5 order closure. This scheme should be nearly unbiased in PBL depth, moisture, and potential temperature according to Coniglio et al. (2013). As land-surface option the Unified Noah land-surface model was used, more information about this option can be found in Ek et al. (2003).

Four subroutines have been implemented in WRF: NO<sub>x</sub> partitioning, NO<sub>x</sub> deposition, NO<sub>x</sub> chemistry and Ozone boundary conditions. The reactions are implemented for each NO<sub>x</sub>, NO<sub>2</sub> and NO emission category (as described in section 3.1.2) in the same way. These subroutines are described below, in section 3.2.2 Implemented subroutines.

### 3.2.1 Domains and resolution

To implement data in WRF, one outer domain and two nested domains were used. The used nesting technique is two-way nesting, which means that there is feedback from the finer to the coarser domain and vice versa. In one-way nesting there is only feedback from the coarser to the finer domain. Misenis and Zhang (2010) who did a five-day summer episode study in the Houston and Galveston region (Texas) for evaluating model performance under different physical parameterizations, horizontal grid spacing, and nesting options found no substantial benefits of two-way nesting over one-way nesting. Fast et al. (2006), however, who modelled air quality in Houston, found better representation of urban and point source plumes with 2-way nesting. For the outer domain (domain 1, d01), an area over the largest part of Europe is taken with a spatial resolution of 20 km x 20 km. This area has been chosen for two reasons: to cover the long term transport of NO<sub>x</sub> and to be able to make a comparison with the satellite data over Europe of TEMIS. For the second domain (domain 2, d02), an area over the Netherlands, as well as the Ruhr area and part Belgium is taken. The domain has a spatial resolution of 4x4 km and will provide most of the advected NO<sub>x</sub> to our main research area: Amsterdam. This domain

---

<sup>3</sup> on July 1st 2013

as well can be compared to satellite data over the Netherlands. For the inner domain (domain 3, d03) an area of 36x32 km<sup>2</sup> is taken around Amsterdam with a spatial resolution of 1x1 km<sup>2</sup>. In Appendix Figure I a picture can be found with the specifications of the different domains.

### 3.2.2 Implemented subroutines

Four subroutines have been implemented to account for different chemistry and NO<sub>x</sub> reaction terms:

- **NO<sub>x</sub> partitioning:**

The NO<sub>x</sub> emissions were partitioned into NO and NO<sub>2</sub>. This subroutine split all the NO<sub>x</sub> emissions directly into 90% NO and 10% NO<sub>2</sub>. These percentages are based on Schultz et al. (2007) and Yao et al. (2005) .

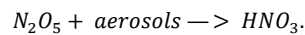
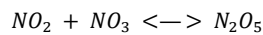
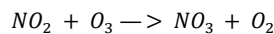
- **NO<sub>x</sub> deposition:**

To take into account the dissipation processes of NO<sub>x</sub> (reaction with OH or O<sub>3</sub> to HNO<sub>3</sub> and deposition), without having to include information on other chemical species, a simple decay reaction is built in the model. Wet deposition is only indirectly taken into account in this way: HNO<sub>3</sub> is very soluble in water and is removed by wet deposition. However, no coupling in the model have been made between precipitation and deposition. The NO<sub>2</sub> in the model is dissipating according to:

$$[NO_2]_n = [NO_2]_{n-1} * e^{\left(\frac{-\Delta t}{\tau}\right)}$$

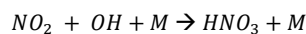
In which  $\Delta t$  is the calculation time step and  $\tau$  the dissipation time constant. The time constant is dependent on the NO<sub>2</sub> termination reactions:

Which are, during night:



For this reaction chain, a  $\tau$  of 24 hours is appropriate (personal communication, Maarten Krol).

During day the main reaction is:



As OH is abundant, this reaction can be regarded as a pseudo first order reaction, i.e. the change in NO<sub>2</sub> concentration with time is only dependent on the OH concentration and the reaction rate constant. The pseudo first order reaction rate constant is  $2.4 * 10^{-11} * (T/300)^{-1.3}$  [cm<sup>3</sup> molecule<sup>-1</sup> s<sup>-1</sup>] (Seinfeld and Pandis, 1998) in which T is expressed in Kelvin. Assuming an average OH concentration of  $1 * 10^6$  molecules/cm<sup>3</sup>, results in a  $\tau$  of 11 hours for the daytime reaction.

In the model, a value of global radiation of 50 W/m<sup>2</sup> is taken as the transition between night-time and daytime reaction regime. With radiation lower than 50 W/m<sup>2</sup>, a  $\tau$  of 24 hours is assumed; otherwise the  $\tau$  is 11 hours.

- **NO<sub>x</sub> chemistry:**

The production/destruction (PD) of NO<sub>2</sub>, NO and O<sub>3</sub> has been built in WRF as the balance between the forward and backward reaction of Equation 1. Similar chemistry reactions have been implemented in modelling studies by Düring et al. (2011) and Berkowicz (2000a).

$$PD = [O_3] * [NO] * k_{19} * dt - [NO_2] * k_5 * dt \quad [mol_n]$$

In which

$$k_{19} = 6.238 * 10^4 * \rho * e^{-1500/T} \quad [mol_{air} * mol_n^{-1} s^{-1}]$$

This reaction constant is based on (Minoura, 1999; Ouwensloot, 2013)

and

$$k_5 = (B_1 * G + B_2 * G^2) * (1 + \alpha) * dt \quad [s^{-1}]$$

$$B_1 = 1.47 * 10^{-5} \quad [W^{-1} m^2 s^{-1}]$$

$$B_2 = 4.84 * 10^{-9} \quad [W^{-2} m^4 s^{-1}]$$

The PD term can be positive: formation of NO<sub>2</sub> and destruction of O<sub>3</sub> and NO, at night this is always the case, as well as negative: destruction of NO<sub>2</sub> and formation of O<sub>3</sub> and NO, the photo dissociation reaction dominates. The global radiation (G) dependent photo dissociation reaction rate k<sub>5</sub> is based on Trebs et al. (2009), which made it possible to implement the reaction rate relatively simple in WRF without information on e.g. solar zenith angle. This reaction constant is validated for the surface only. However, according to Seinfeld and Pandis (1998), the photo dissociation reaction constant is 8\*10<sup>-3</sup> s<sup>-1</sup> at surface and 10\*10<sup>-3</sup> s<sup>-1</sup> at 30 km height. So, it seems not to change much with height and could probably be used safely for all heights, as we have done in this study.

The air density (ρ) in kg/m<sup>3</sup> and temperature (T) in Kelvin are prescribed by WRF for every x,y,z location of the grid cells, albedo (α) [-] and G [W/m<sup>2</sup>] are specified for each column, and do not differ with z.

Reactions with other compounds, as volatile organic compounds, are not considered.

- **Ozone boundary conditions:**

Ozone was implemented in the model by describing its boundary and initial conditions. After this, ozone can be spread by WRF and used in the chemistry, so it can be broken down and formed freely. The model domains can be seen as large boxes, as depicted in Figure 3. The inner box is the modelled domain 1. In this inner box, everywhere above 3 km height, ozone is assumed in this domain to be 35 ppb constantly. This is done using a subroutine which loops over all layers above 3 km and set them to 35 ppb.

WRF uses a boundary layer around the four sides of this modelling box, depicted as the outer box, where the boundary conditions for meteorology and chemistry variables were set mainly for advection. The boundary conditions set for ozone are 30 ppb on all four sides (the pink colour in the picture (only shown on the backside)). During a WRF run the concentrations of d01 around d02 make up boundary conditions for d02 and those of d02 those for d03. In the initial conditions for domain 1 as well as for domains 2 and 3, ozone was set to 30 ppb.

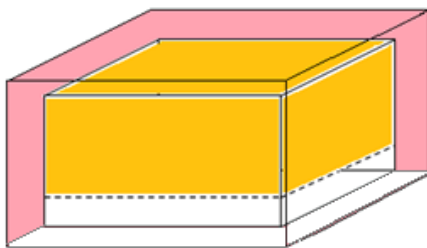


Figure 3 Simple description of domain 1 (inner box) and its boundaries (outer box).

### 3.3 Data preparation for WRF

For running WRF terrain information (static data) as well as meteorological input information (grib data) is required. The NCEP data was ungridded so it could be read in WRF and combined with the geogrid data processed with metgrid, which prepared the data so it could be used in the three nested domains. With Real.exe input and boundary conditions were made for model runs with WRF. In Figure 4 an overview of the pre-processing can be found. To run WRF-chem tracer species were specified and prepared in Real.exe and emission data was provided to WRF for every domain.

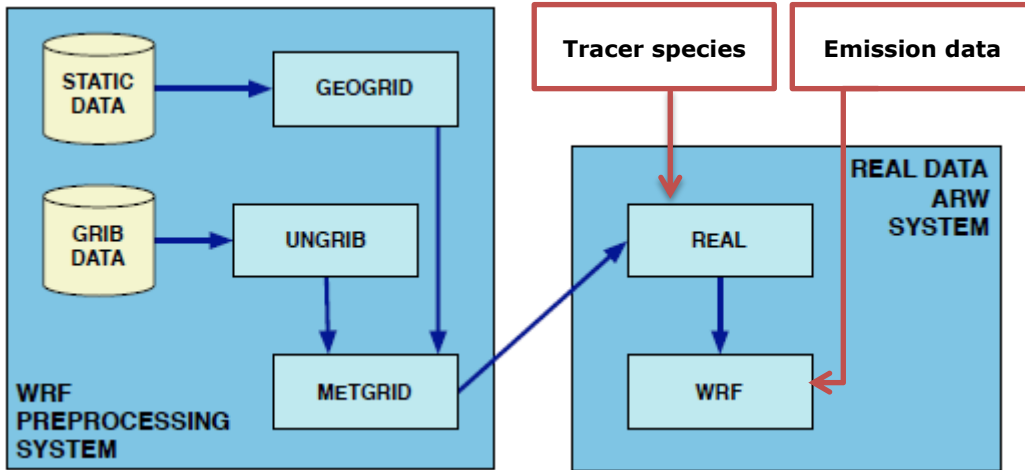


Figure 4 Structure of data and programs in the WRF pre-processing system (WPS) and ARW system. Adapted from: (Skamarock et al., 2008).

### 3.3.1 providing chemistry input

The MACC database with the original grid of  $1/8^\circ$  lon x  $1/16^\circ$  lat, was re-gridded to be able to use in WRF. This was done as follows for every modelled period:

1. the MACC area emission data were re-gridded to a grid which was readable for WRF;
2. the emissions were interpolated to  $1 \times 1 \text{ km}^2$  scale;
3. the locations of the point sources were calculated and added to the WRF  $1 \times 1 \text{ km}^2$  grid;
4. for domain 2 and 3 the  $1 \times 1 \text{ km}^2$  grid cells were aggregated;
5. emission dates were specified as well as the emission time step (1h);
6. monthly, day-of-the-week and hourly emission time factors were applied, calculated back to UTC, to provide hourly specified emissions;
7. these emissions were written to a NetCDF file, which WRF could read.

### 3.3.2 Implementing more refined $1 \times 1 \text{ km}^2$ emissions

For Amsterdam, the emissions have been specified on the  $1 \times 1 \text{ km}^2$  grid. For refining the emissions from  $8 \times 8 \text{ km}^2$  further to  $1 \times 1 \text{ km}^2$ , the  $\text{NO}_x$  emissions of road traffic categories (701, 702 and 703) have been modified in the input file. The data was extracted and by using multiplication factors to the original  $8 \times 8 \text{ km}^2$  emission, specified on the  $1 \times 1 \text{ km}^2$ . These factors were based on the NSL monitoring tool ([www.nsl-monitoring.nl](http://www.nsl-monitoring.nl)) and information on the location of the highways (Figure 6).

The information of the NSL monitoring tool together with road information led to the emission maps shown in Figure 7.



Figure 6a Screenshot of calculated  $\text{NO}_2$  concentrations along roads in the centre of Amsterdam according to the NSL monitoring tool (<https://www.nsl-monitoring.nl/viewer/>)



Figure 6b Google maps showing highways and N-ways over large Amsterdam

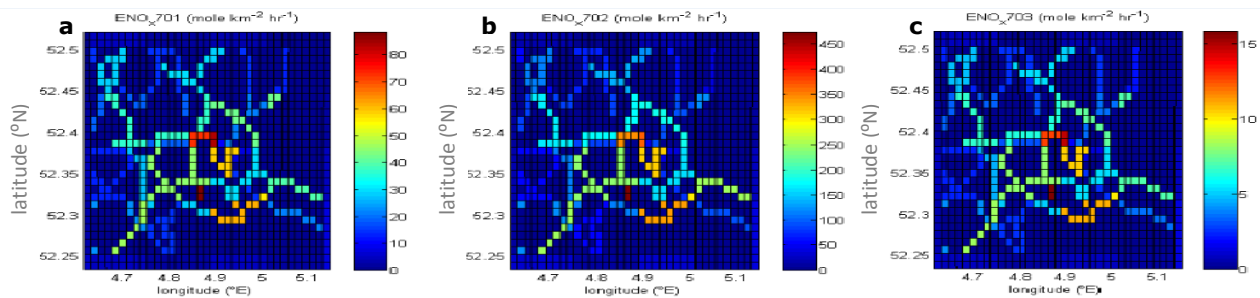


Figure 7 Emissions on d03 scaled to a  $1 \times 1 \text{ km}^2$  grid for (a) category 701, (b) category 702 and (c) category 703

### 3.4 Commuters' Exposure

To investigate the influence of bicycling time and weather on the  $\text{NO}_2$ -exposure of commuters, two main routes were chosen, based on the driving directions Google maps suggested (route 1a and 2a). Besides these main routes, for each route, a commonly taken alternative cycling way was included (route 1b and 2b). In Figure 8 the routes have been depicted.

Routes 1a (length: 11.9 km) and 1b (12.3 km) are east-west orientated and have as starting point the student dormitory "ACTA", Louwesweg 1, Amsterdam. The end point is at the science location of the University of Amsterdam "UVA science park", address: Science Park 904b, Amsterdam.

Routes 2a (10.4 km) and 2b (12.3 km) are south-north orientated and start at a central point in Amstelveen, address: Graaf Aelbrechtlaan 99, the end point is the Amsterdam Central Station, route 2b follows for a large part the Amstel river.

All routes follow for a large part the most intense used bicycle routes, i.e. roads were more than 1500 cyclist pass through during evening rush hours (16u - 18u LT), according to the Service Infrastructure, Traffic and Transport of the municipality Amsterdam (Figure 8a ; DIVV, 2012b).

The length of the route through each grid cell of d03 has been estimated. The  $\text{NO}_2$  concentration [ $\text{gNO}_2/\text{l}$  air] in the grid-cell at the specific time was multiplied with the length value in the specific grid cell, the time it took to ride that length, and the minute ventilation of a cyclist, summing this up for all crossed grid cells resulted in a total amount of inhaled  $\text{NO}_2$  in grams during the ride. For the different situations, the amounts were calculated relative to the a-variant of the route on 8h LT.

The average cycling speed in the city is 15 km/h including stops while waiting for traffic lights (Zuurbier et al., 2009). So 4 minutes is taken to ride 1 km.

Different studies have been done on minute ventilations, i.e. the amount of air inhaled per unit of time of cyclist. The minute ventilation is dependent on different factors as the cycling speed, the age, breast volume, sex and condition of the cyclist and can be as high as 120 l/min under high effort (Morree et al., 2011). Zuurbier et al. (2009) found an average minute ventilation of 23.5 l/min. However, they measured for a somewhat lower average cycle speed of 12 km/h. In the article of Zuurbier it is mentioned that in a study of Vrijkotte, 1990, where unlimited speed was used, a minute ventilation of 29.1 l/min was found. Therefore, in our study, a minute ventilation of 29.1 l/min was used.

The situations that are evaluated to compare the amount of inhaled  $\text{NO}_2$  are a 'winter day': March 25, a spring day: April 23 and two summer days: July 10 and July 22. The days have been chosen based on the high  $R^2$  values for  $\text{NO}_2$  during rush hours.

March 25, July 8 and July 22 were Mondays; July 10 was a Wednesday.

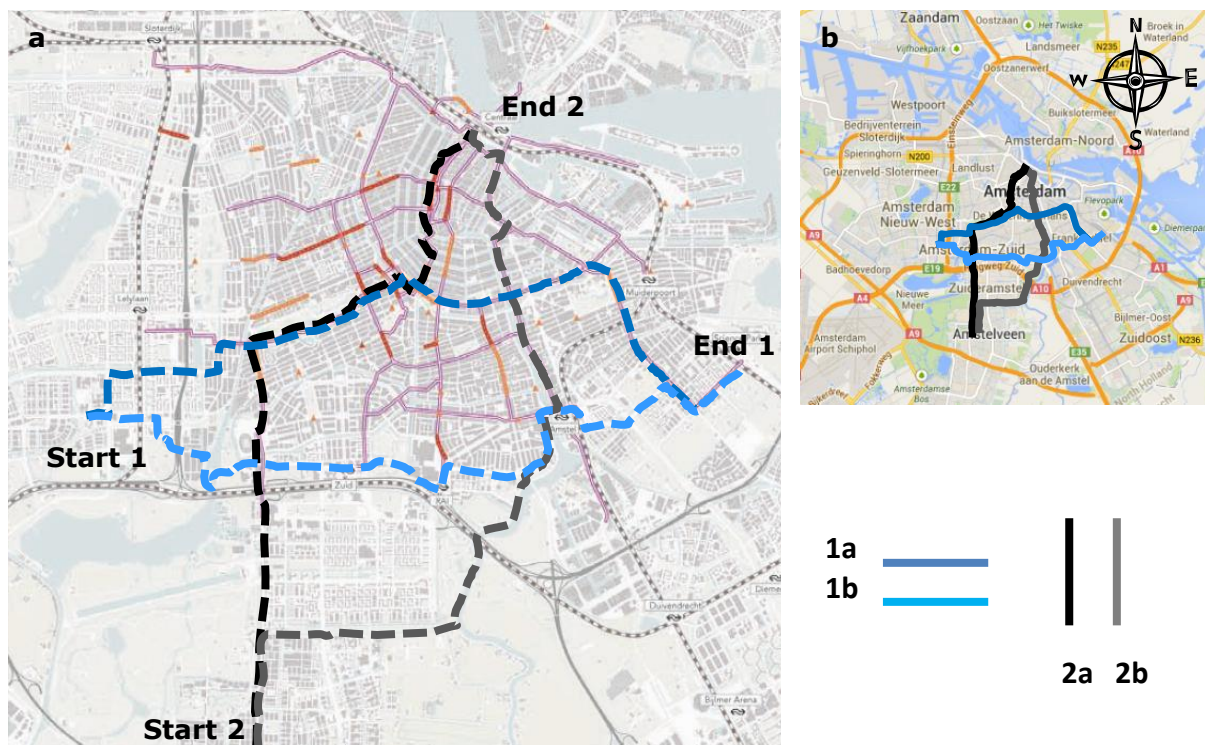


Figure 8 (a) Cycling routes over the map of the busiest cycle roads of Amsterdam (>1500 cyclist in the evening rush hours, 16h - 18h LT, each day; pink lines). Source: (DIVV, 2012b). (b) Cycling routes with respect to the (high) ways in Amsterdam

### 3.5 Satellite comparison

The satellite comparison is made by comparing the WRF model output with data from a service that the European Space Agency (Cyrys et al.) offers: the Tropospheric Emission Monitoring Internet Service (TEMIS). TEMIS provides tropospheric  $\text{NO}_2$  columns, which are derived from satellite observations and a KNMI combined modelling/retrieval/assimilation approach. The skew column  $\text{NO}_2$  data of the Ozone Monitoring Instrument (OMI), converted to vertical columns are derived by KNMI/NASA (Boersma et al., 2007). We used the Dutch OMI  $\text{NO}_2$  (DOMINO) data product version 2.0 for comparison.

Between 11 and 15 UTC 3 or 4 satellite orbits are done over Western Europe. These datasets were combined: the most reliable satellite observation data of around 11.30 for the Netherlands were kept, and places which were not covered by this satellite were filled with data of the other two or three orbit's data. From this dataset the  $\text{NO}_2$  tropospheric column data was used, as well as the centre longitudes and latitudes and the four corner longitudes and latitudes of each data point. With the corner coordinates, polygons were made and filled with the associated  $\text{NO}_2$  values. Subsequently the polygon data were interpolated to the grid of either domain 1 (8x8 km grid) or 2 (4x4 km grid), by looking for the satellite centre longitudes that lay to the utmost 0.5 degree latitude and 0.25 degree longitude off of the latitude and longitude of the WRF grid. This was done to prevent large satellite polygons being assigned to much more WRF grid cells than the small satellite polygons, while the small polygons contain the most reliable values.

For July 8 of the grid cells used, the maximum cloud fraction was 23.3%; for March 27 this was 32.0%.

### 3.6 Implementation of the different runs

Runs for different meteorological situations have been done, to make it possible to investigate the influence of weather on commuters' exposure and to investigate the model performance under different meteorological situations. In Table 3 an overview of the circumstances during the different runs can be found back. In choosing the different situations, the emphasis was on model performance differences

with temperature, wind direction and sun hours per day. All days were days without precipitation, as wet deposition is not directly taken into account in this study.

**Table 3 All dates are in 2013; no precipitation is been registered on the days that have been chosen. The stated temperatures are mean temperatures measured by KNMI<sup>4</sup> for Schiphol airport.**

wind direction	sun hours	>25°C	>18°C	5°C -15°C	<10°C
(North)-Easterly	<b>&gt; 9 hours of sun</b>	21-24 July	6-9 July	--	25-28 March
	<b>&lt; 5 hours of sun</b>	--	10-13 July	--	--
	<b>varied</b>	--	--	19-22 April	--
(South)-Westerly	<b>varied</b>	--	--	22-25 April	--

---

<sup>4</sup> The Royal Dutch Meteorological Institute: <http://knmi.nl/klimatologie/daggegevens/index.cgi>

## 4. Results

### 4.1 Validation of the model for temperature and NO<sub>2</sub>

WRF represents the daily temperature cycle very well (Figures 9, 10), but underestimates the values by around two degrees (Table 4). As well night time as day time temperatures are underestimated, but whether the largest underestimation is at night or during day differs for the modelled periods. For the summer days 6-9 July the night-time underestimation is largest, for the spring days 22-25 April, the daytime underestimation is higher. However, the measured temperatures on other city stations lay often closer to the modelled temperatures (Figure 9, 10). For the summer period the day-time temperatures lay in the GGD measurement range; the consistency of WRF with measurements increases from 6 to 9 July (Figure 9). For the spring days 22 – 24 April the consistency with observations decreases with time (Figure 10). On the used statistic methods to test the performance of the model for temperature, the period of 21 – 24 July compares best to observations, 22 – 24 April worst (Table 4).

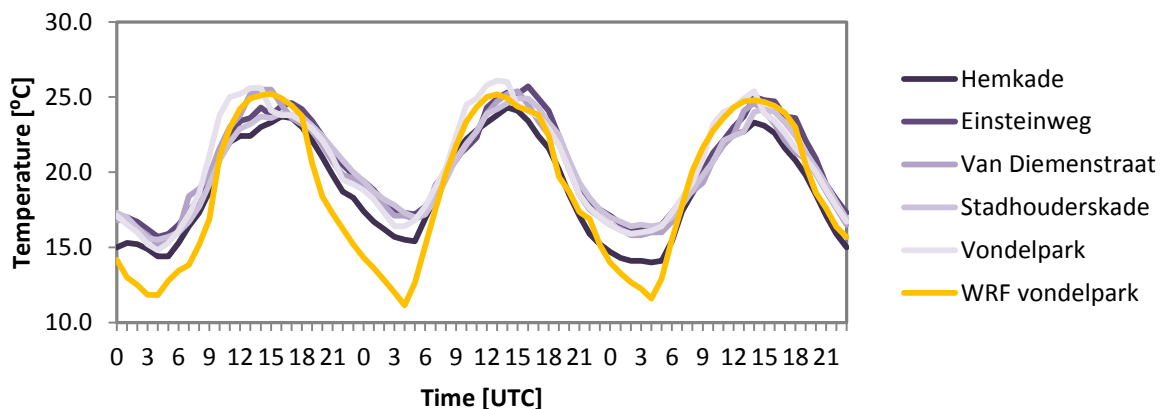


Figure 9 Temperature in degree Celsius on the GGD stations (purple lines) and modelled with WRF (yellow line) for three days: between 6 July 00h and 9 July 00h.

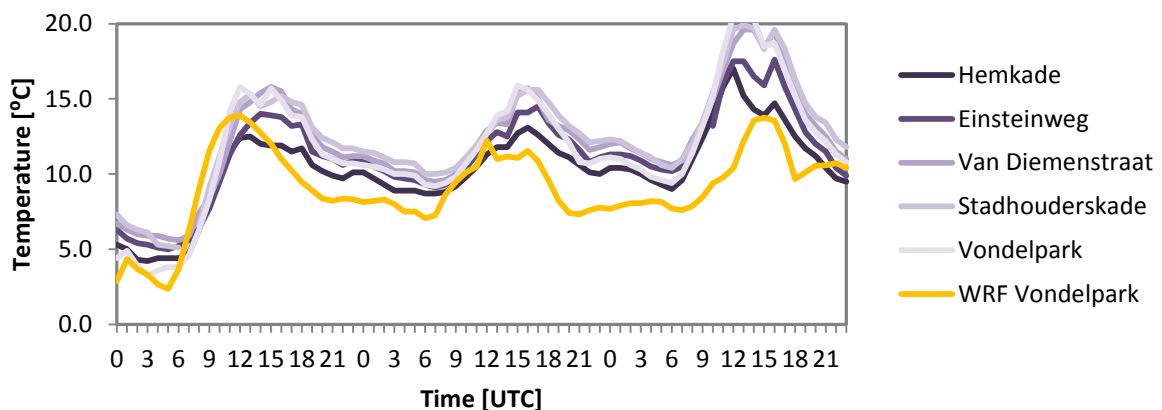


Figure 10 Temperature in degree Celsius on the GGD stations (purple lines) and modelled with WRF (yellow line) for three days: between 22 April 00h and 25 April 00h.

The mean bias error (MBE), which is the average difference between the observed (O) and modelled or predicted (P) values, varied for temperature between a model underestimation of 1.7 and 2.7 (Table 4). The unbiased variance ( $s_d^2$ ) also called the average noise factor, discriminated even stronger between the modelled days. In Table 4 an overview of the statistics on the difference between modelled and observed temperature with as well the root mean square error (RMSE), and the systematic and unsystematic proportions or magnitudes ( $MSE_u/MSE$  and  $1 - MSE_u/MSE$  respectively). It is clear that in all cases except 19-22 April the systematic proportion of the error was larger than the unsystematic error (Table 4). These statistics have been calculated according to (Willmott, 1982).

Table 4 Quantitative comparison between Vondelpark modeled and observed temperature for different runs. The terms N, MSE<sub>s</sub>/MSE, 1- MSE<sub>s</sub>/MSE and R<sup>2</sup> are dimensionless, the others have unit degree Celsius

T modeled vs observed	N*	O	P	MBE			s <sub>d</sub> <sup>2</sup>	RMSE	R <sup>2</sup>	MSE <sub>s</sub> /MSE	1- MSE <sub>s</sub> /MSE
				all	night	day					
25 - 27 March	71	1.50	-1.26	-2.7	-3.3	-2.3	1.96	3.10	0.765	0.92	0.08
19 - 22 April	72	8.67	6.57	-2.1	-1.8	-2.4	1.64	2.44	0.841	0.43	0.67
22 - 24 April	72	11.8	9.09	-2.7	-2.3	-3.1	4.87	3.48	0.706	0.82	0.18
6 - 8 July	72	20.5	18.8	-1.7	-1.9	-1.5	3.08	2.40	0.921	0.71	0.29
10 - 12 July	71	16.8	14.8	-2.0	-1.9	-2.0	0.80	2.18	0.837	0.72	0.28
21 - 24 July	72	25.9	24.0	-1.9	-2.4	-1.4	1.86	2.36	0.930	0.68	0.32

\*N is the number of temperature observations over the three run days.

The ability of the model to capture the NO<sub>2</sub> concentrations differed by day. In general the model gave high R squared (R<sup>2</sup>) values for the background stations Vondelpark, Sportpark Ookmeer and Oude Schans Centrum: up to 0.84 (Table 5). For the rush hours the model in general gave somewhat higher correlations, the worst results are found for daytime: between 9-13 UTC (not shown). The average concentrations of 21 and 22 July were closest to the observed values, but the R<sup>2</sup> values of these days were low. In general WRF underestimated the NO<sub>2</sub> concentrations, especially at the first run day (Table 6). An underestimation is even more evident when comparing the model with busy traffic locations as Einsteinweg (not shown); a maximum concentration of 91 µg/m<sup>3</sup> was measured for example during the period of 6-9 July, while the maximum concentration that WRF reached was 60 µg/m<sup>3</sup> for location Einsteinweg during this period.

Table 5 R<sup>2</sup> and average (difference) in NO<sub>2</sub> for the different modelled days over 24 hours for 4 different stations: background stations Vondelpark, Sportpark Ookmeer and Oude Schans Centrum, and traffic location Stadhouderskade. The average NO<sub>2</sub> concentrations and differences are in [µg/m<sup>3</sup>] and are taken over all 4 locations.

Date (2013)	R <sup>2</sup> NO <sub>2</sub>				
	Vondelpark	Sportpark Ookmeer	Oude Schans	Stadhouderskade	Average
25 March <sup>1</sup>	0.40	0.78	0.47	0.45	<b>0.52</b>
26 March	0.52	0.39	0.28	0.30	<b>0.37</b>
27 March	0.61	0.54	0.62	0.27	<b>0.51</b>
19 April <sup>1</sup>	0.01	0.01	0.01	0.23	<b>0.06</b>
20 April	0.00	0.24	0.08	0.05	<b>0.09</b>
21 April	0.09	0.00	0.02	0.24	<b>0.09</b>
22 April <sup>1</sup>	0.02	0.25	0.08	0.00	<b>0.09</b>
23 April	0.54	0.67	0.57	0.21	<b>0.50</b>
24 April	0.81	0.85	0.63	0.02	<b>0.58</b>
6 July <sup>1</sup>	0.84	0.78	0.10	0.02	<b>0.43</b>
7 July	0.47	0.42	0.41	0.60	<b>0.47</b>
8 July	0.04	0.05	0.60	0.37	<b>0.27</b>
10 July <sup>1</sup>	0.60	0.47	0.22	0.13	<b>0.35</b>
11 July <sup>2</sup>	0.26	0.12	-	0.24	<b>0.21</b>
12 July <sup>2</sup>	0.02	0.34	-	0.43	<b>0.26</b>
21 July <sup>1</sup>	0.06	0.73	0.16	0.01	<b>0.24</b>
22 July	0.37	0.06	0.26	0.46	<b>0.29</b>
23 July	0.01	0.00	0.46	0.03	<b>0.13</b>
average	<b>0.32</b>	<b>0.37</b>	<b>0.31</b>	<b>0.23</b>	<b>0.31</b>
week	<b>0.32</b>	<b>0.35</b>	<b>0.38</b>	<b>0.24</b>	<b>0.32</b>
weekend	<b>0.29</b>	<b>0.43</b>	<b>0.15</b>	<b>0.18</b>	<b>0.27</b>

<sup>1</sup>Data of 00h UTC was excluded from the comparison this day, on these times WRF was still on its initial conditions

<sup>2</sup>The Oude Schans measurements lack for this day

The  $R^2$  shows the explained variance and it emphasises peak (mis)matches, as the difference between the modelled and observed values is squared (Legates and McCabe, 1999). It however does not show whether the relation between the modelled and observed values is negative or positive. Therefore, as well the correlation coefficient is calculated. As the  $R^2$  squares the error,  $R^2$ s of above 0.25 do already give a moderate relation between modelled and observed values, while CCs only of  $>0.5$  do give a moderate relation (Doorn and Rhebergen, 2006).

Correlation coefficients (CCs) have been calculated according to:

$$CC = \frac{\sum(x_i - \bar{x})(y_i - \bar{y})}{\sqrt{\sum(x_i - \bar{x})^2} * \sqrt{\sum(y_i - \bar{y})^2}}$$

In which  $x_i$  is the modelled concentration on time  $i$ ,  $y_i$  is the measured concentration on time  $i$  and  $\bar{x}$  and  $\bar{y}$  the average modelled and measured values.

In Table 6 and Table 7 an overview of the correlation coefficients for  $\text{NO}_2$  and NO can be found. Highest CCs were found for the background stations. For  $\text{NO}_2$  CCs of on average 0.6 and 0.7 were found for 25-27 March and April 23 and 24. The highest CC found for  $\text{NO}_2$  is 0.92 for July 6. WRF performed less on the other days. Negative correlations have even been found for the periods of April 19-22, July 6-8 and for the Stadhouderskade on July 22 and 23. For NO the CCs were higher, on average the CC of NO is 0.49. But also for NO negative correlations were found (Table 7).

**Table 6 Correlation coefficients of  $\text{NO}_2$  compared to measurements of Vondelpark, Oude Schans, Stadhouderskade and Sportpark Ookmeer over 24 hours. The number of observations (N) differed station and day between 21 and 24, see Appendix Table I. Acronyms: Von = Vondelpark, Ook=Sportpark Ookmeer, OS=Oude Schans Centrum, StdK=Stadhouderskade.**

Date (2013)	Correlation Coefficient $\text{NO}_2$					Average $\text{NO}_2$ conc [ $\mu\text{g}/\text{m}^3$ ]		
	Von	Ook	OS	StdK	Ave rage	WRF	GGD	diff
25 March <sup>1</sup>	0.75	0.88	0.69	0.54	<b>0.71</b>	4.86	16.51	-11.65
26 March	0.74	0.63	0.53	0.50	<b>0.60</b>	6.12	19.32	-13.20
27 March	0.73	0.73	0.79	0.52	<b>0.69</b>	9.95	26.59	-16.64
19 April <sup>1</sup>	0.03	-0.12	-0.18	0.32	<b>0.01</b>	18.65	24.34	-5.69
20 April	-0.05	0.49	0.32	-0.23	<b>0.13</b>	10.10	18.35	-8.25
21 April	0.28	0.06	0.14	0.49	<b>0.24</b>	27.64	25.88	1.76
22 April <sup>1</sup>	0.15	0.50	0.28	-0.04	<b>0.22</b>	28.93	41.63	-12.70
23 April	0.73	0.78	0.76	0.48	<b>0.69</b>	32.07	28.38	3.69
24 April	0.90	0.92	0.79	0.20	<b>0.70</b>	36.10	35.83	0.27
6 July <sup>1</sup>	0.92	0.88	0.32	0.14	<b>0.57</b>	12.68	17.83	-5.15
7 July	0.71	0.64	-0.65	-0.77	<b>-0.02</b>	15.13	17.04	-1.91
8 July	0.21	0.22	-0.78	-0.53	<b>-0.22</b>	13.54	15.72	-2.18
10 July <sup>1</sup>	0.77	0.69	0.46	0.50	<b>0.61</b>	9.96	16.07	-6.11
11 July <sup>2</sup>	0.50	-0.34		0.54	<b>0.23</b>	7.15	14.37	-7.22
12 July <sup>2</sup>	0.09	0.58		0.22	<b>0.30</b>	-	-	-
21 July <sup>1</sup>	0.70	0.88	0.69	0.21	<b>0.62</b>	16.69	16.68	0.01
22 July	0.61	0.25	0.51	-0.68	<b>0.17</b>	33.37	31.69	1.68
23 July	0.15	0.03	0.47	-0.63	<b>0.00</b>	25.99	42.75	-16.76
average week	<b>0.50</b>	<b>0.48</b>	<b>0.32</b>	<b>0.10</b>	<b>0.35</b>	<b>18.17</b>	<b>24.06</b>	<b>-5.89</b>
weekend	<b>0.49</b>	<b>0.44</b>	<b>0.39</b>	<b>0.15</b>	<b>0.37</b>	<b>18.89</b>	<b>26.10</b>	<b>-7.21</b>
weekend	<b>0.51</b>	<b>0.59</b>	<b>0.16</b>	<b>-0.03</b>	<b>0.31</b>	<b>16.49</b>	<b>19.16</b>	<b>-2.71</b>

<sup>1</sup>Data of 00h UTC was excluded from the comparison this day, on these times WRF was still on its initial conditions

<sup>2</sup>Oude Schans measurements lack for this day

Table 7 Correlation coefficients and average (difference) of NO compared to measurements of Vondelpark, Oude Schans, Stadhouderskade and Sportpark Ookmeer over 24 hours. The number of observations (N) differed per station and day between 21 and 24, see Appendix Table I. Acronyms: as named in Table 6.

Date (2013)	Correlation Coefficient NO					Average NO conc [ $\mu\text{g}/\text{m}^3$ ]		
	Von	Ook	OS	StdK	Ave rage	WRF	GGD	diff
25 March <sup>1</sup>	0.40	0.72	0.75	0.55	<b>0.60</b>	2.51	3.19	-0.68
26 March	0.30	0.65	0.31	0.70	<b>0.49</b>	2.88	3.68	-0.80
27 March	0.21	0.72	0.71	0.65	<b>0.57</b>	3.67	4.48	-0.81
19 April <sup>1</sup>	0.27	0.41	0.23	0.31	<b>0.30</b>	6.00	6.44	-0.45
20 April	-0.08	-0.09	-0.18	-0.09	<b>-0.11</b>	3.34	4.19	-0.86
21 April	0.31	0.34	0.09	0.34	<b>0.27</b>	9.31	5.74	3.57
22 April <sup>1</sup>	0.82	0.70	0.93	0.73	<b>0.80</b>	13.72	13.64	0.08
23 April	-0.13	0.52	0.15	0.14	<b>0.17</b>	11.99	7.28	4.71
24 April	0.94	0.75	0.92	0.88	<b>0.87</b>	25.39	13.81	11.58
6 July <sup>1</sup>	0.70	0.79	0.77	0.25	<b>0.63</b>	4.85	3.22	1.64
7 July	0.66	0.59	0.50	0.42	<b>0.54</b>	5.10	4.47	0.64
8 July	0.71	0.74	0.74	0.84	<b>0.76</b>	5.31	5.31	0.00
10 July <sup>1</sup>	0.47	-0.03	0.61	0.30	<b>0.34</b>	3.43	3.74	-0.31
11 July <sup>2</sup>	0.38	0.71		0.68	<b>0.59</b>	2.74	3.11	-0.37
12 July <sup>2</sup>	0.00	-0.13		0.13	<b>0.00</b>	4.53	4.57	-0.05
21 July <sup>1</sup>	0.01	0.68	0.12	0.23	<b>0.26</b>	5.98	2.69	3.29
22 July	0.76	0.91	0.94	0.54	<b>0.79</b>	19.89	5.26	14.64
23 July	0.71	0.72	0.94	0.59	<b>0.74</b>	17.03	5.61	11.42
average	<b>0.41</b>	<b>0.54</b>	<b>0.53</b>	<b>0.46</b>	<b>0.49</b>	<b>8.20</b>	<b>5.58</b>	<b>2.62</b>
week	<b>0.45</b>	<b>0.57</b>	<b>0.66</b>	<b>0.54</b>	<b>0.55</b>	<b>9.16</b>	<b>6.16</b>	<b>3.00</b>
weekend	<b>0.32</b>	<b>0.46</b>	<b>0.26</b>	<b>0.23</b>	<b>0.32</b>	<b>5.72</b>	<b>4.06</b>	<b>1.66</b>

<sup>1</sup>Data of 00h UTC was excluded from the comparison this day, on these times WRF was still on its initial conditions

<sup>2</sup>Oude Schans measurements lack for this day

## 4.2 Sensitivity analysis

To investigate how sensitive the model was to the given input and boundary conditions for ozone, the input and boundary conditions were halved (from 30 ppb and 35 ppb to 15 ppb and 17.5 ppb) and doubled (to 60 and 70 ppb). For March 25-27, where the modelled O<sub>3</sub> concentration fluctuated on the normal run between 44 and 64  $\mu\text{g}/\text{m}^3$  the halving of the O<sub>3</sub> boundary conditions and input lead to a 54% lower O<sub>3</sub> concentration, to a 18% lower NO<sub>2</sub> and to a 30% higher NO concentration (Table 8). For April 22-24, where modelled ozone concentrations fluctuated between 0.04 and 65  $\mu\text{g}/\text{m}^3$ , the halving of the O<sub>3</sub> boundary conditions and input lead to a 62% lower O<sub>3</sub> concentration, and to a 35% lower NO<sub>2</sub> and 49% higher NO concentration (Table 8). During night, the differences were found smaller than during daytime.

Changing the partitioning factors of NO<sub>x</sub> emission from NO<sub>2</sub>:NO = 10%:90% to NO<sub>2</sub>:NO = 25%:75% led to a decrease of 22% in NO for 22-24 April and a 12% decrease in NO for 25-27 March. NO<sub>2</sub> increased with 17% and 9% for these periods respectively and O<sub>3</sub> increased with 19% and 2% for these periods.

Table 8 Factor NO<sub>x</sub> and O<sub>3</sub> concentrations between halving/doubling ozone input and boundary conditions and 'normal' NO<sub>x</sub> and O<sub>3</sub> values and changing NO<sub>x</sub> emission partitioning (from NO<sub>2</sub>:NO = 10%:90% to NO<sub>2</sub>:NO = 25%:75%) . Factors did hardly differ between stations, average is taken over Vondelpark and Stadhouderskade.

	halving ozone input			doubling ozone input			NO <sub>x</sub> emission = 25% NO <sub>2</sub> (was 10% NO <sub>2</sub> )		
	NO	NO <sub>2</sub>	O <sub>3</sub>	NO	NO <sub>2</sub>	O <sub>3</sub>	NO	NO <sub>2</sub>	O <sub>3</sub>
25-27 March	1.30	0.82	0.46	0.69	1.11	2.13	0.88	1.09	1.02
22-24 April	1.51	0.65	0.38	0.49	1.38	2.87	0.78	1.17	1.19

### 4.3 Spatial patterns

The model not only enables the possibility to look at differences on time, it enables as well to look at differences in space. With the very fine one km grid of the first domain, the NO and NO<sub>2</sub> plumes and the places with high concentrations are visualized (Figure 11). Advection plumes of the Amsterdam Western Port area, Schiphol airport and the Industrial area of IJmuiden are recognisable as well as the ring way of Amsterdam. The high concentrations in the south-east of the smallest domain are probably caused by a combination of emissions of the power plant in Muideren and shipping over the Amsterdam-Rijn canal and the IJmeer. The high concentrations over the North-sea are found because of the minimal development of a mixed layer over this wet area, leading to very limited vertical mixing. Advection of sea air will, consequently, not lead to high concentrations over land, as the concentrations are then rapidly mixed in the vertical. In total column concentrations, hence this pattern of high concentrations over the North-sea is not found back, while the places with high concentration over land are.

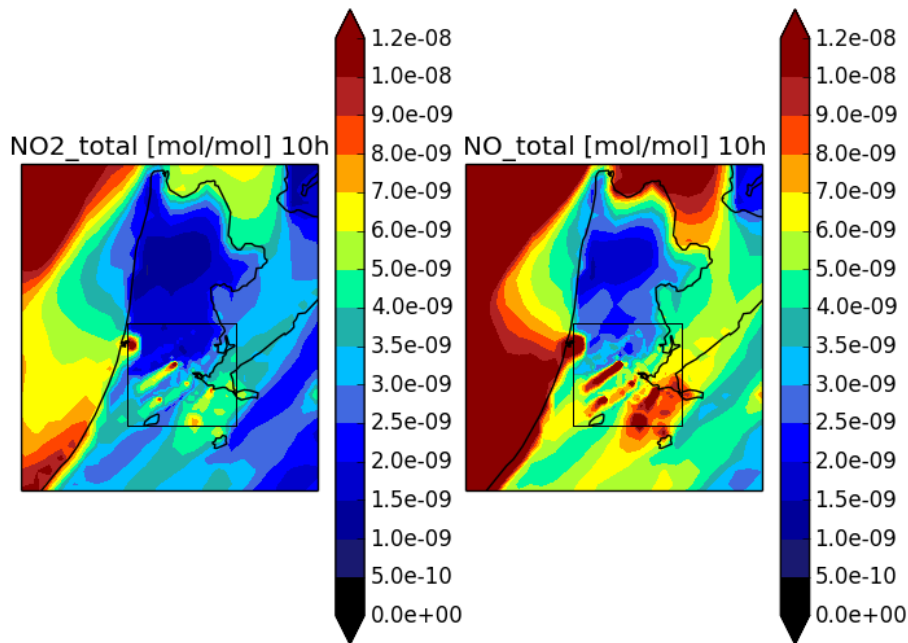


Figure 11 NO and NO<sub>2</sub> concentrations [mol/mol] over Amsterdam, for part of domain 2 and domain 3. The black rectangle frames d03. WRF ground layer, July 8 12h LT

### 4.4 Daily patterns in NO<sub>x</sub> for different weather situations

In general, the daily observed cycle of NO<sub>2</sub> in the city can be described as high values in the morning around 8 am local time (LT), somewhat or much lower concentrations during the day, and a (sometimes less distinct) evening peak around 23h LT (Figure 12). The NO cycle can be described as a morning peak around 8 am LT and low concentrations during the rest of the day and during the night (Figure 14). WRF captures the average daily cycle of NO<sub>2</sub> concentration on weekdays quite well. It, however, underestimates the morning peak (Figure 13). For weekend days the model seems to underestimate the morning peak as well, and predicts it too early in the morning. The evening values are overestimated (Figure 13). For NO, the model underestimates the morning peak as well, especially on weekdays, besides, WRF tends to find a small evening peak as well, while this is not found back in the measurements (Figure 14/15). The average daily pattern of NO<sub>2</sub> matches for weekdays better than for weekend days. For NO the model does not perform better for weekdays.

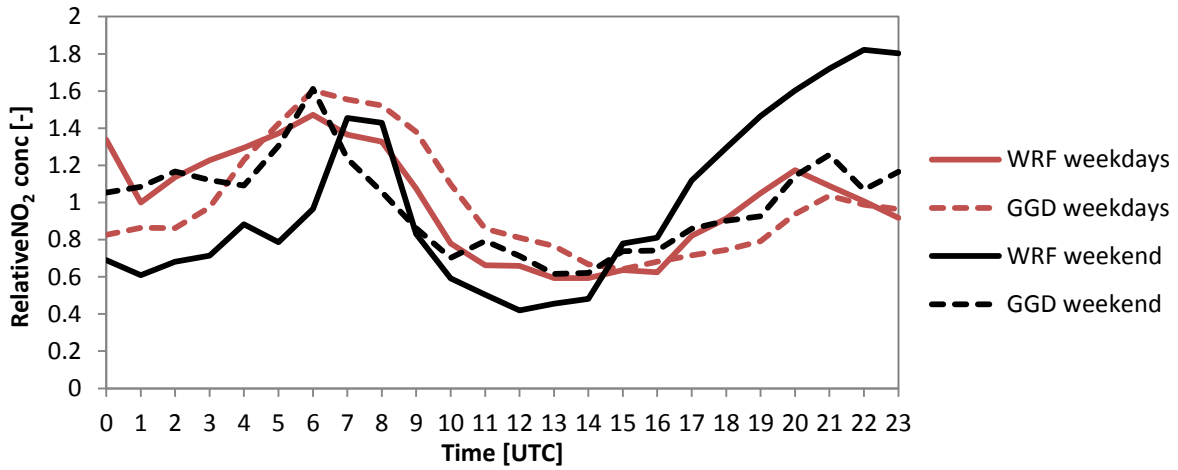


Figure 12 Relative average daily cycle of  $\text{NO}_2$ , location: Vondelpark. Averaged over weekend days: Saturday and Sunday (N=7), and weekdays: Monday, Tuesday, Wednesday, Friday (N=8) – no Thursday has been in the modelled days.

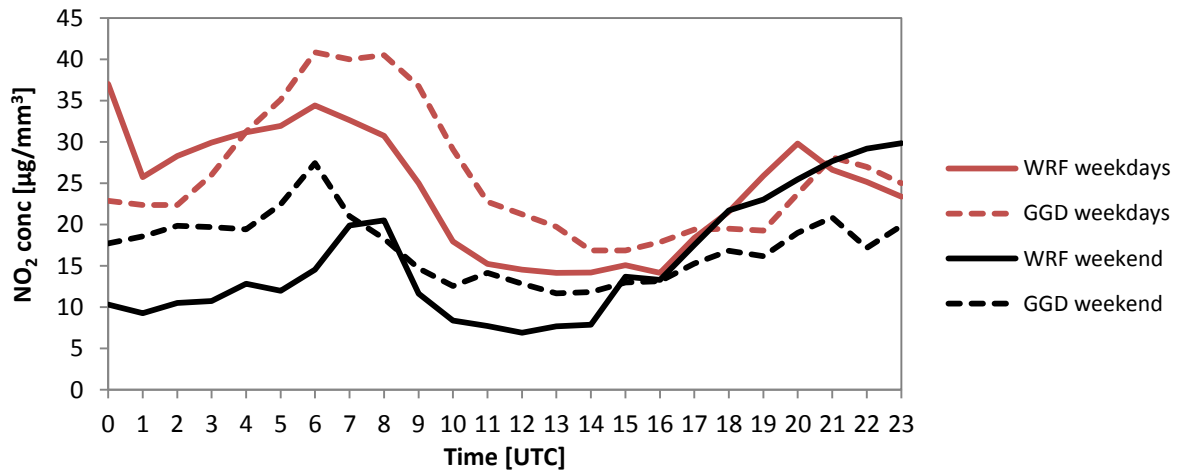


Figure 13 Average daily cycle of  $\text{NO}_2$ , location: Vondelpark. Averaged over weekend days: Saturday and Sunday (N=7), and weekdays: Monday, Tuesday, Wednesday, Friday (N=8).

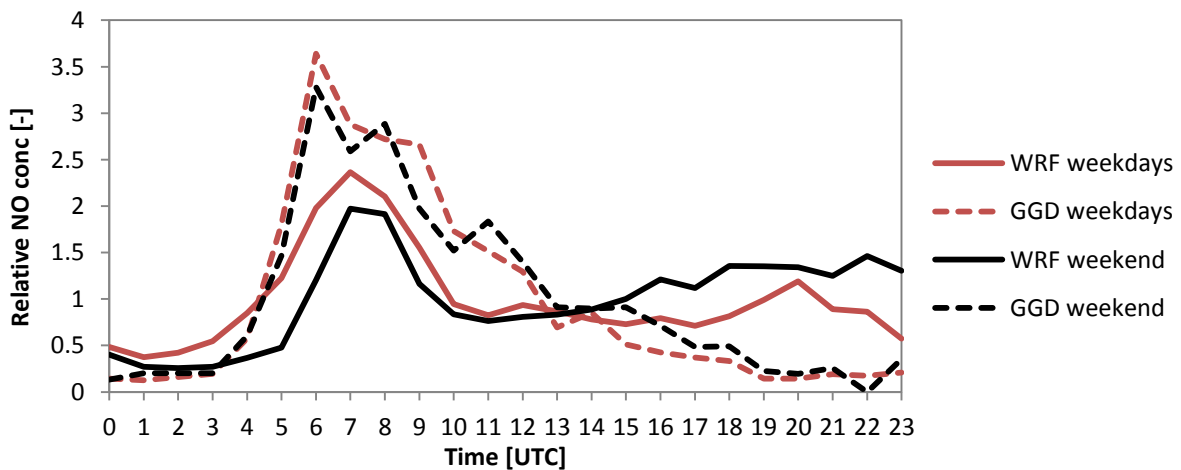


Figure 14 Relative average daily cycle of  $\text{NO}$ , location: Vondelpark. Averaged over weekend days: Saturday and Sunday (N=7), and weekdays: Monday, Tuesday, Wednesday, Friday (N=8).

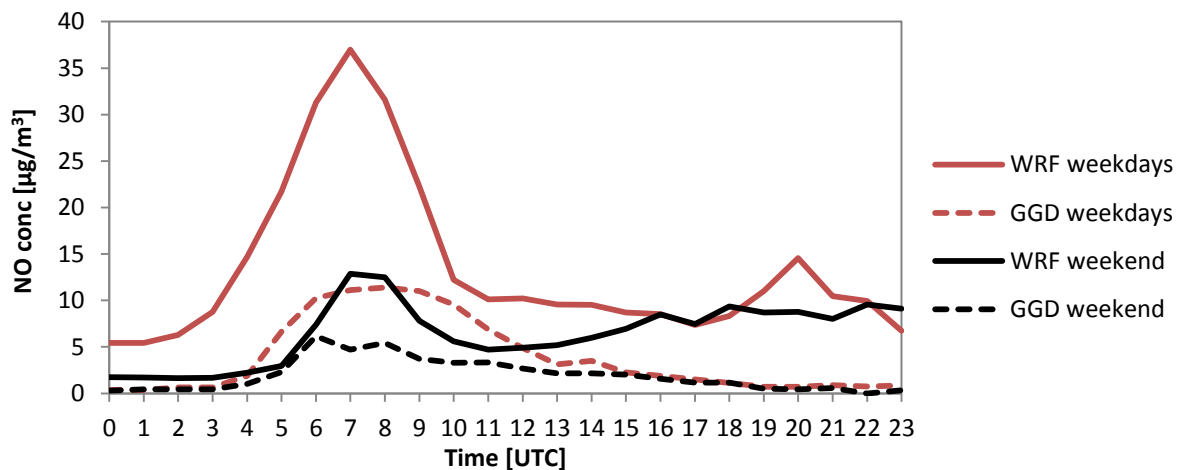


Figure 15 Average daily cycle of  $\text{NO}_2$ , location: Vondelpark. Averaged over weekend days: Saturday and Sunday (N=7), and weekdays: Monday, Tuesday, Wednesday, Friday (N=8)

The model represented the NO and  $\text{NO}_2$  concentrations for the run of April 22 to 24 quite well for the urban background station Vondelpark. For the traffic station Stadhouderskade the concentrations were comparable as well, but somewhat underestimated (Figures 16, 17). For 25 – 27 March the  $\text{NO}_2$  concentrations are clearly underestimated, the NO concentrations are better represented than the  $\text{NO}_2$  concentrations (Figures 18,19).

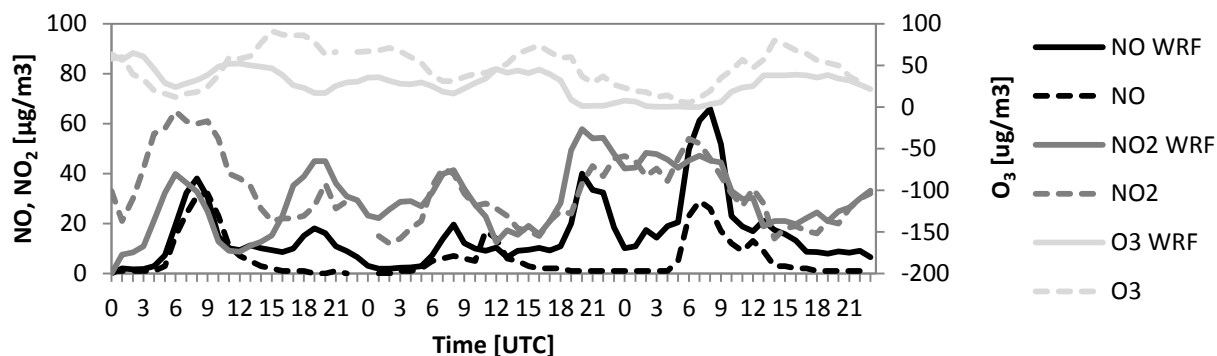


Figure 16 For location Vondelpark: NO,  $\text{NO}_2$  and  $\text{O}_3$  concentrations – last mentioned are plotted on the secondary y-axis - in micrograms per cubic meter on 22, 23 and 24 April 2013. Solid lines are modelled values, dotted lines are measurements of the particular days.

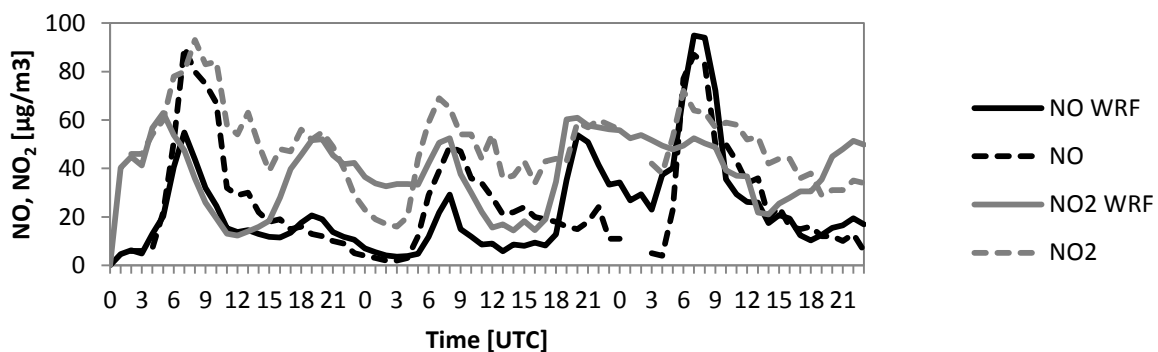


Figure 17 For location Stadhouderskade: NO,  $\text{NO}_2$  and  $\text{O}_3$  concentrations in micrograms per cubic meter on 22, 23 and 24 April 2013. Solid lines are modelled values, dotted lines are measurements of the particular days.

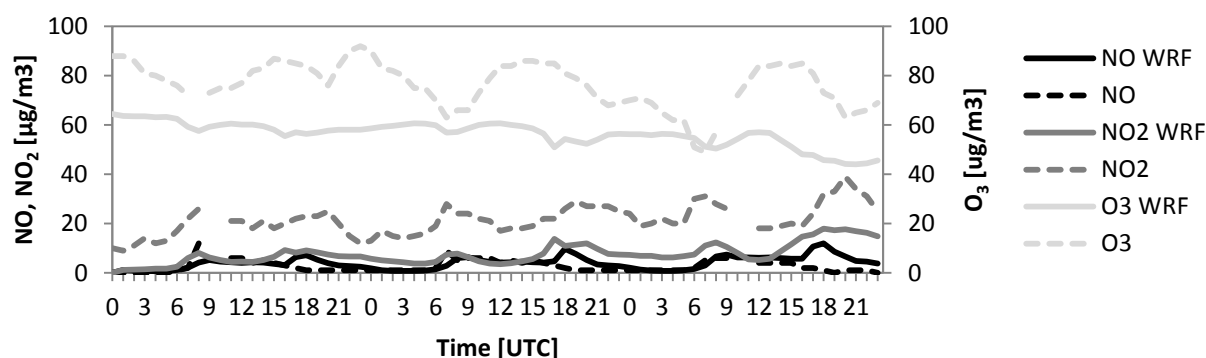


Figure 18 For location Vondelpark: NO, NO<sub>2</sub> and O<sub>3</sub> concentrations – last mentioned are plotted on the secondary y-axis - in micrograms per cubic meter on 25, 26 and 27 March 2013. Solid lines are modelled values, dotted lines are measurements of the particular days.

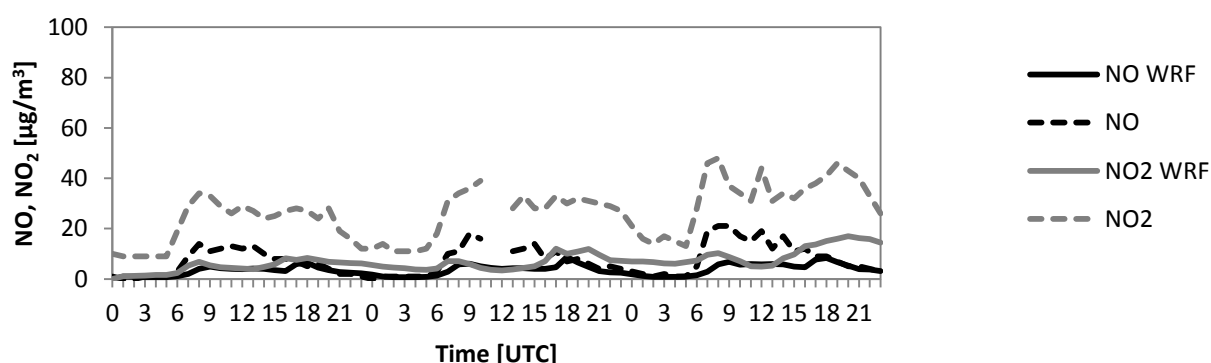


Figure 19 For location Stadhouderskade: NO, NO<sub>2</sub> and O<sub>3</sub> concentrations in micrograms per cubic meter on 25, 26 and 27 March 2013. Solid lines are modelled values, dotted lines are measurements of the particular days.

#### 4.5 Commuters' exposure

Different meteorological situations have been compared to investigate the influence of weather on the NO<sub>2</sub> exposure. As the model sometimes underestimated, sometimes overestimated the absolute values, but the pattern of the daily cycle was captured well, a comparison of relative concentrations is done. The R squared of the model compared to four representative stations as a bulk, are varying between 0.23 for March 25 and 0.52 for April 23; for the Vondelpark station only, the R<sup>2</sup> were found about two times higher (Table 9). All exposure in Tables 10 and 11 values have been compared to the exposure values when leaving 8 a 'clock in the morning. In Table 12 the 100% exposure values for the four days can be found.

Table 9 R squared (R<sup>2</sup>) of model compared (for bicycle times 5-8 UTC and 14-17 UTC) to measurements on four stations: Oude Schans, Stadhouderskade, Sportpark Ookmeer and Vondelpark together, as well as only Vondelpark.

		March 25	April 23	July 10	July 22
Four city stations	N	32	32	30	32
	R <sup>2</sup>	0.2317	0.5176	0.3358	0.3832
Vondelpark	N	8	8	8	8
	R <sup>2</sup>	0.5671	0.9313	0.6865	0.7504

March 25 is the only situation where the afternoon values exceeded the morning values. The earlier the departure - except for the latest morning departure -, in the morning as well as in the afternoon, the lower the inhaled concentrations of NO<sub>2</sub> are. The latest afternoon ride of route 1a causes 2.3 times as much exposure as the one in the early morning. Another striking point is that the concentrations inhaled at route 2b are 1.02 times those of route 2a, while in all other weather situations route 2a has somewhat lower exposure values than route 2b. On the other hand, the 1b concentrations are very clearly higher than the route 1a concentrations (Table 10a).

**Table 10a Commuters' exposure on March 25 for routes 1a, 1b, 2a and 2b. The percentages are taken relative to 1a 8h for routes 1 and to 2a 8h for routes 2. Time is LT.**

	Route 1a	Route 1b	Route 2a	Route 2b
7h	62%	112%	65%	68%
8h	100%	144%	100%	98%
9h	109%	145%	106%	94%
10h	88%	117%	80%	71%
16h	111%	156%	103%	98%
17h	131%	195%	133%	131%
18h	137%	216%	141%	145%
19h	144%	217%	144%	151%

**Table 10b Commuters' exposure on April 23 for routes 1a, 1b, 2a and 2b. The percentages are taken relative to 1a 8h for routes 1 and to 2a 8h for routes 2. Time is LT.**

	Route 1a	Route 1b	Route 2a	Route 2b
7h	83%	90%	82%	112%
8h	100%	107%	100%	131%
9h	109%	116%	115%	149%
10h	101%	110%	108%	139%
16h	40%	40%	41%	54%
17h	43%	43%	45%	58%
18h	39%	44%	41%	58%
19h	56%	64%	65%	89%

On April 23, the afternoon concentrations are around 40% of the morning concentrations. The best departure time in the morning is still 7 am LT, but the differences with other morning departure times are smaller. In the afternoon, the difference between leaving at 16, 17 or 18 pm LT are at max 4%. Leaving at 19 pm LT still gives the highest values. The differences between route 1a and 1b are very small, route 2b gives 1.3 times as high exposure values (Table 10b).

July 10 and July 22 are two summer situations. For these days, lowest exposure was found for a departure at 8 am on July 10 and 10 am on July 22, and for the afternoon on 4 pm LT. Highest exposures are found on 7 am LT; in the afternoon the highest exposures are on 7 pm LT. For July 10 the difference between route 1a and 1b is much higher than for July 22. This is as well true for the difference between route 2a and 2b. Another point important to mention is that on July 22, the exposure values decrease with time during the morning. This is not so or less clearly observed during one of the other

**Table 11a Commuters' exposure on July 10 for routes 1a, 1b, 2a and 2b. The percentages are taken relative to 1a 8h for routes 1 and 2a 8h for routes 2. Time is LT.**

	Route 1a	Route 1b	Route 2a	Route 2b
7h	136%	158%	108%	150%
8h	100%	111%	100%	125%
9h	102%	111%	100%	123%
10h	114%	128%	110%	147%
16h	29%	35%	26%	35%
17h	36%	43%	30%	43%
18h	56%	63%	42%	60%
19h	61%	74%	53%	79%

**Table 11b Commuters' exposure on July 22 for routes 1a, 1b, 2a and 2b. The percentages are taken relative to 1a 8h for routes 1 and 2a 8h for routes 2. Time is LT.**

	Route 1a	Route 1b	Route 2a	Route 2b
7h	112%	113%	111%	127%
8h	100%	101%	100%	113%
9h	91%	92%	91%	103%
10h	73%	73%	73%	82%
16h	44%	45%	41%	47%
17h	36%	40%	40%	41%
18h	44%	48%	45%	46%
19h	58%	61%	54%	67%

runs.

To put the modelled days in perspective of yearly average values and do as well get a picture of exposure values for the entire day, we will give an indication of average yearly NO<sub>2</sub> concentrations. On the modelled days, the average measured NO<sub>2</sub> concentration for the urban background stations Vondelpark, Oude Schans Centrum and Sportpark Ookmeer was 21.3 µg/m<sup>3</sup>, for the traffic station Stadhouderskade, the average NO<sub>2</sub> concentration was 34.8 µg/m<sup>3</sup>. Over 2014, the average concentrations for the aforementioned urban background stations was 25.9 µg/m<sup>3</sup>, for the Stadhouderskade 39.8 µg/m<sup>3</sup>. The modelled periods were on average thus periods of relative low NO<sub>2</sub> concentration.

**Table 12 100% exposure values in mg for the different routes on the different days**

	100% exposure [mg]	
	route 1	route 2
<b>March 25</b>	7.48	8.18
<b>April 23</b>	56.47	44.75
<b>July 10</b>	16.75	15.03
<b>July 22</b>	57.83	51.42

#### 4.6 Satellite comparison

The comparison is done for two minimally cloudy days in which the satellite orbits passed the Netherlands more than once: July 8 and March 27. For July 8 the model and satellite data are well comparable and show similar dispersion plumes and sources (Figure 20, 21). On average the model underestimates the NO<sub>2</sub> values, for d01 with  $0.12 \cdot 10^{15}$  molec/cm<sup>2</sup>, for d02 with  $0.63 \cdot 10^{15}$  molec/cm<sup>2</sup>. The average NO<sub>2</sub> concentration found by the satellite is  $1.828 \cdot 10^{15}$  molec/cm<sup>2</sup>, WRF found an average of  $1.440 \cdot 10^{15}$  molec/cm<sup>2</sup>. More than 90% of the d01 data has an error of within  $2.5 \cdot 10^{15}$  molec/cm<sup>2</sup>, for d02 this is 70% of the data (see as well Figure 22). The largest differences are found over the centre of the UK, where WRF modelled two spots with high NO<sub>2</sub> concentration, while on the satellite data only one spot is found and near the Ruhr-area: the Ruhr plume is more spread by WRF, this gives underestimations of concentrations around South-Limburg, and overestimated concentrations in central Belgium (Figure 20, 21).

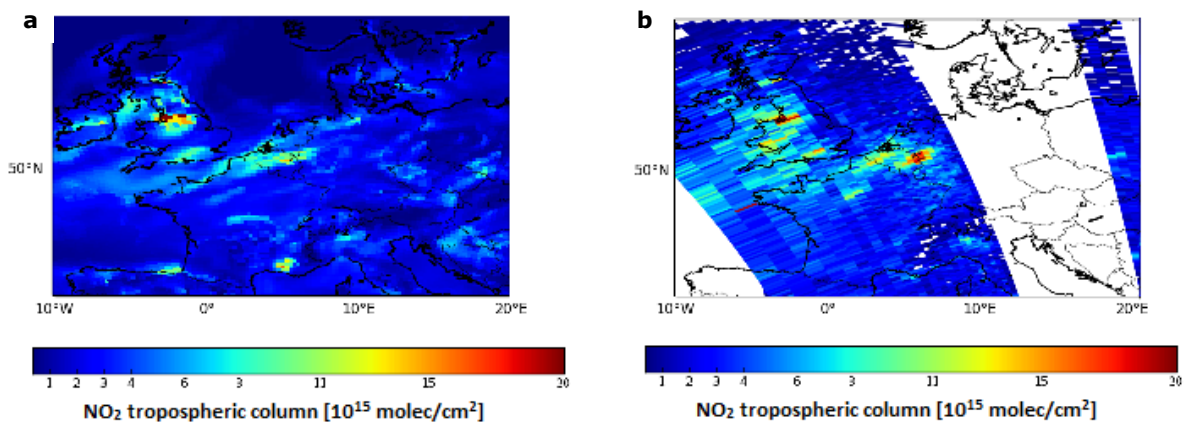


**Figure 20 Modelled NO<sub>2</sub> concentrations (a) and satellite observed NO<sub>2</sub> concentrations (b) for the tropospheric column [molec/cm<sup>2</sup>], around 12 am, July 8 2013.**

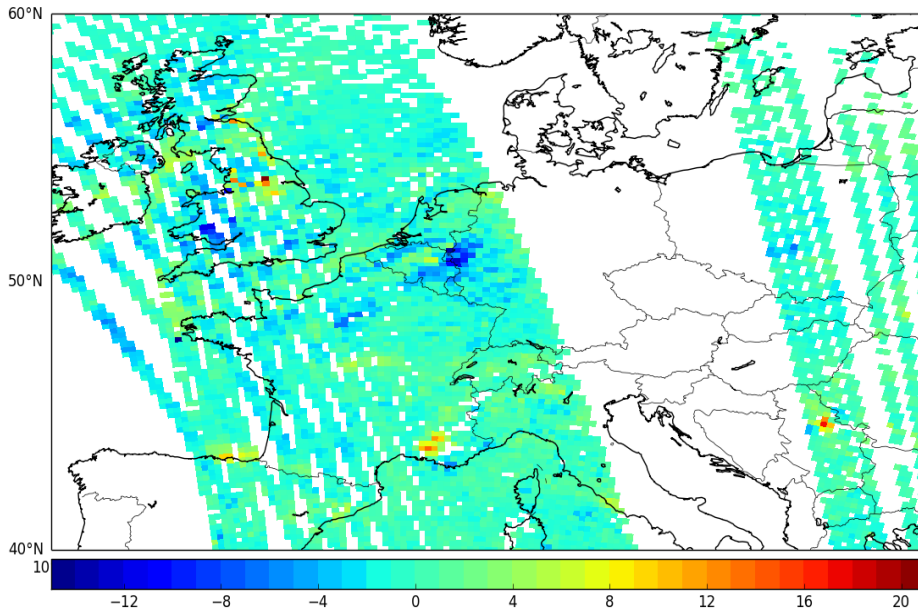


Figure 21 NO<sub>2</sub> difference in tropospheric column for d01 July 8 2013 [ $10^{15}$  molec/cm<sup>2</sup>]

For March 27, a comparison is done as well. The NO<sub>2</sub> concentrations modelled for d02 were on average  $7.6 \cdot 10^{15}$  molec/cm<sup>2</sup> lower than the satellite values. Part of the reason for this underestimation could be a too low conversion of NO to NO<sub>2</sub> with the low temperatures on March 27: when adding the modelled NO to NO<sub>2</sub> and comparing the sum to the NO<sub>2</sub> concentrations found by the satellite, the resulting difference for each percentile is very alike the difference found for d02 on July 8 (Figure 22). In the Appendix Figure II a scatter plot of the modelled versus observed values can be found for July 8.

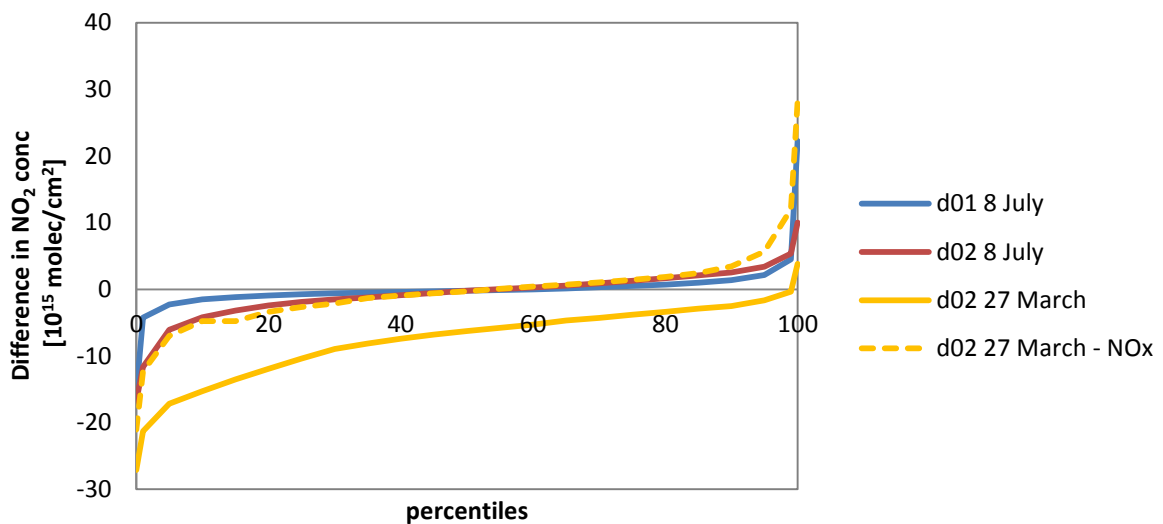


Figure 22 Difference in NO<sub>2</sub> concentration (model minus satellite) for percentiles of the data of domains 1 and 2 of July 8 and for domain 2 of March 27 NO<sub>2</sub> as well as NO+NO<sub>2</sub> compared to satellite NO<sub>2</sub> data.

## 5. Discussion

### 5.1 Validation

The temperature calculated by WRF is representing the daily cycle very well, however, WRF systematically underestimates the temperature by around two degrees, somewhat stronger during night time than during daytime in the results of March and July but not in April. The underestimation of temperature by WRF is probably partly caused by the heat-island effect. The urban heat island is as well strongest during night-time (see Arnfield (2003) for a review study on heat-islands). As the urban modelling scheme of WRF is not used, a very simple urban parameterization is used now, which is mainly based on the land-use differences causing a shift in the energy budget, decreasing latent and increasing sensible heat fluxes. This does not take into account the emission of heat by buildings and could thus underestimate the UHI.

Besides, the problem can lay in the model. Several other studies reported cold biases in WRF (Case et al., 2008; Cheng and Steenburgh, 2005; Misenis and Zhang, 2010; Zhang et al., 2009), the reason of this biases is not totally clear, but seems to occur most by local closure schemes (Stensrud, 2007), in this study the local closure scheme MYNN is used.

The negative temperature bias could lead to underestimation of the amount of NO converted into NO<sub>2</sub>, as Equation 1 (page 4) from left to right is faster with higher temperatures. For March 25-27, where as well temperature as NO<sub>2</sub> concentrations were most underestimated, it is tempting to say that there is a link between the two factors. However, the NO concentrations were underestimated as well for this period (with on average 0.76 µg/m<sup>3</sup>), so the solution must be sought elsewhere – think about too high mixture in the vertical or too low advection terms. This could also be concluded from the fact that temperature underestimations were equally high for 22-24 April, while for April 23 and 24 there is an overestimation of NO<sub>2</sub> as well as for NO.

From the used equation to calculate the reaction constant for the NO<sub>2</sub> forming reaction, it could be seen that the temperature dependence is according to:  $e^{-1500/T}$ . This means that with an average temperature of around zero degree Celsius, so 273 Kelvin, as is the case on 25-27 March the rate constant increases with 4% for a 2 degrees higher temperature. For temperatures of around 25 degree Celsius, the increase is only 3% per 2 degrees higher temperature. As higher NO<sub>2</sub> concentrations as well lead to higher backward reaction speed, and lower NO concentrations to lower forward reaction speeds, it could be said that the 2 degrees underestimation of WRF is not a large problem for simulating chemical reaction rates.

Despite the simple chemistry in the model and the too low ozone concentrations, the NO and NO<sub>2</sub> concentrations follow most of the time the right daily cycle and the order of magnitude of the model is comparable with the measured values. WRF is particularly good in explaining the variation measured at background stations as Vondelpark and Sportpark Ookmeer. For a high traffic station as the Einsteinweg, the concentrations are highly underestimated, in particular during rush hours. Of all runs, the April 22-24 NO<sub>2</sub> concentrations were best comparable to observed values, the concentrations of March 25-27 worst.

The cause of the average underestimation of NO<sub>x</sub> on traffic stations is probably the scale difference: concentrations are given by WRF as an average over the lowest grid box, which has dimensions of 1km x 1km x 39 meters and the emissions are on 1x1 km<sup>2</sup> scale for traffic, and for other sources, the emission resolution was even 8x8 km<sup>2</sup> resolution. The measurements of GGD are point measurements on a height of around 2.5 meter. The traffic station will thus measure the direct emissions from traffic hotspots, while the model gives more of an average value of long-range transport, regional emissions and urban emissions on kilometre scale. A nice overview of the sources of air pollution in a city can be found in Figure 23 (Kakosimos et al., 2010). It looks like the model is particularly able to represent the urban background concentrations and not to represent the traffic hotspots.

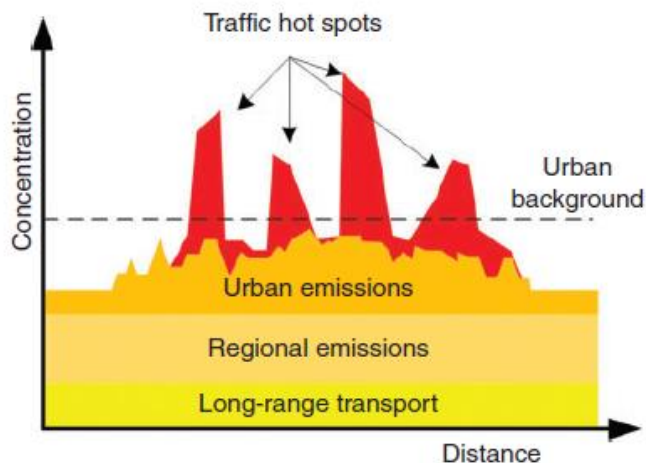


**Figure 23** “ Schematic illustration of the air pollutant contribution from long-range transport, regional emissions, the city area and the street traffic. The relative magnitude of the various contributions depends on the considered pollutant and the actual dispersion conditions (governed by the meteorology).” Source: Kakosimos et al. (2010).

For NO<sub>2</sub> in general the first modelled day was found to have the largest underestimation; this could be because WRF needs spin-up time and the pollutant concentrations need to build up from zero at 00h. For NO, the underestimation on the first day was not present, as the model periods started at 00 UTC, and during the night the NO concentrations already are close to zero.

In general WRF underestimated the NO<sub>2</sub> concentrations and overestimated the NO concentrations. In March, the underestimation was found largest and it occurred in both NO and NO<sub>2</sub> concentrations. This could be due to several reasons: WRF could have been overestimating the mixed layer depth on the windy day and the vertical mixing of WRF was too high, leading to too low ground-level concentrations. Another explanation could be that the NO<sub>x</sub> transport was underestimated. On March 25-27 the boundary layer grew in WRF from 550 meter during night to 850 meter during day. The strong easterly probably prevents the development of a stable boundary layer at night. So, concentrations are quite well mixed all the time, leading to low surface concentrations. As the wind speed is high these days, advection becomes more important in determining the NO<sub>x</sub> concentrations and an underestimation of the NO<sub>x</sub> advection could as well play a role in the underestimation. The general pattern of underestimating NO<sub>2</sub> while overestimating NO can be explained by either a too low fraction that is emitted as NO<sub>2</sub> compared to NO, as that factor was found important in the sensitivity analysis for NO<sub>x</sub> partitioning, or due to a too low reaction speed of the reaction from NO to NO<sub>2</sub>. In the results of the sensitivity analysis for changing the emission fraction, it is shown that the model showed large differences when the fraction NO<sub>2</sub> is made higher.

WRF clearly has difficulties representing the concentrations during the very warm days of 21 to 23 July. Especially for the traffic station Stadhouderskade, the measured NO<sub>2</sub> concentrations do not follow the usual daily cycle on these days: the highest concentrations are found during the day and are lower in the late afternoon and night (Figure 24). On top of that, the measured concentrations do clearly build up by day. For July 22 and 23 2013, the RIVM gave a warning for moderate smog (RIVM, 2013c). Summer smog only occurs when there is enough sunshine, combined with a stable boundary layer. WRF represents these days as a 'normal' hot summer day: with a lot of buoyancy due to the high temperatures and a high well mixed boundary layer causing concentrations to be low during daytime. In reality, the boundary layer is more stable, causing emissions to accumulate around the place of emission, as is seen in the observations (Figure 24). The NO cycle is better followed by WRF on these days, probably because in normal cases NO already is very emission dependent.

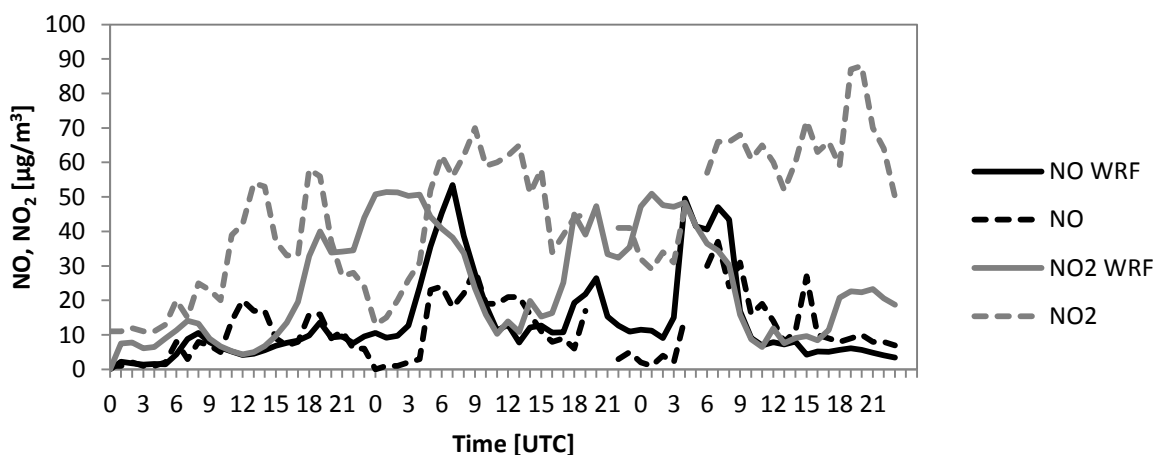


Figure 24 For traffic location Stadhouderskade: NO, NO<sub>2</sub> and O<sub>3</sub> concentrations in micrograms per cubic meter on 21, 22 and 23 July 2013. Solid lines are modelled values, dotted lines are measurements of the particular days.

As found in the sensitivity analysis for ozone, there is no 1:1 relationship between higher O<sub>3</sub> concentrations and higher NO<sub>2</sub> and lower NO concentrations (Table 8). However, the model is still quite sensitive to ozone concentrations, the reaction speed of Reaction 1 is dependent on the concentrations of ozone, NO and NO<sub>2</sub>. From the found factors of ozone, NO and NO<sub>2</sub> under different ozone input conditions (Table 8), we deduced general equations for both periods used for the sensitivity analysis to investigate the effect of implementing the real ozone concentration instead of the underestimated modelled value:

$$25-27 \text{ March: } \begin{aligned} \text{NO factor} &= 0.17 * (\text{O}_3 \text{ factor})^2 - 0.80 * (\text{O}_3 \text{ factor}) + 1.63 \\ \text{NO}_2 \text{ factor} &= -0.14 * (\text{O}_3 \text{ factor})^2 + 0.54 * (\text{O}_3 \text{ factor}) + 0.60 \end{aligned}$$

$$22-24 \text{ April: } \begin{aligned} \text{NO factor} &= 0.22 * (\text{O}_3 \text{ factor})^2 - 1.13 * (\text{O}_3 \text{ factor}) + 1.91 \\ \text{NO}_2 \text{ factor} &= -0.15 * (\text{O}_3 \text{ factor})^2 + 0.76 * (\text{O}_3 \text{ factor}) + 0.38 \end{aligned}$$

For March 25-27, the modelled O<sub>3</sub> concentrations were 0.7 times the measured O<sub>3</sub> concentrations. When this number is used in the equation for March, the NO concentrations for March 25-27 would be 16% higher, and the NO<sub>2</sub> would be 10% lower. For 22-24 April, the modelled O<sub>3</sub> concentrations were 0.6 times the measured O<sub>3</sub> concentrations, this would lead to 31% higher NO concentrations and 21% lower NO<sub>2</sub> concentrations. This, however, is only the averaged shift. As ozone concentrations are mainly underestimated during day time, the differences in concentrations should as well be larger on day time than during night. The lower NO<sub>2</sub> concentrations, however, would not improve the model, as on average for both periods the NO<sub>2</sub> concentrations are already underestimated. This suggests that the reaction speed of the temperature dependent reaction of NO with O<sub>3</sub> to NO<sub>2</sub> is too low, or the speed of radiation dependent reaction backward is too high.

In general, NO was overestimated during night. This night time overestimation of NO was found also in the study of Zhang et al. (2009) where a fully implemented WRF-chem model was used for modelling chemical species in Mexico city. As the boundary layer is more stable during night than during day and emissions are spread over a smaller volume, the accuracy of the predicted boundary layer height is more critical at night.

Equal to our study, the study of Zhang et al. (2009) found higher daytime correlations than night-time correlations for temperatures as well as NO and NO<sub>2</sub>. Overall a correlation coefficient (Legates and McCabe) of 0.45 and 0.43 was found in the study of Zhang et al. (2009) for NO and NO<sub>2</sub> respectively. In our study NO and NO<sub>2</sub> CCs were on average 0.49 and 0.35 but varying, from negative CCs to CCs of 0.94 for NO and of 0.92 for NO<sub>2</sub>. For NO highest CCs were found in the period of 6-8 July, for NO<sub>2</sub> highest correlation was found on April 23 and 24. The day time NO<sub>2</sub> correlation coefficients found by Zhang et al. were 0.55, the night time 0.43. On average daytime correlation coefficients in our study for NO<sub>2</sub> were 0.41, night time correlation coefficients 0.32. Also a better performance for weekdays than for weekend days was found in both their and our study. This is expected, as weekdays have higher emissions and thus more clear daily patterns.

There is, however, a difference in comparing all observations as a bulk, as is probably done in the study of Zhang et al. (2009) and comparing each station and day apart as is done in our study. Each station has its own distinct pattern, based on the distance of the stations to the emission sources. If the model works right, better correlation should be found comparing the stations apart than as a bulk. This is in our study generally the case (compare Table 6 and Appendix Table III). When all stations were compared as a bulk, for example, weekday CCs were on average 0.32 and weekend correlation coefficients 0.13. When the correlation is calculated, however, for each station apart the average CCs show not such a clear difference between week and weekend days: the average CC for weekdays is 0.37 and for weekend days 0.31: apparently the differences between the stations are larger in the weekends than on weekdays. Another remark is that the study of Zhang et al. (2009) is performed in Mexico City, where the concentrations were on average  $71 \mu\text{g}/\text{m}^3$  and daily patterns will be much more distinct than in Amsterdam. This leads probably earlier to higher correlation coefficients.

Misenis and Zhang (2010) who did a five-day summer episode study in the Houston and Galveston region (Texas) for evaluating model performance under different physical parameterizations, horizontal grid spacing, and nesting options, looked as well to the model performance for NO and NO<sub>2</sub>. Unfortunately, they only mentioned the normalized mean bias and no R<sup>2</sup> or correlation coefficient. Their normalized mean bias varied between +54.9% and +242% for NO<sub>2</sub> and between -59.2% and -80.2% for NO, dependent on which parameterization scheme, way of nesting and resolution was used. In our study, the mean bias error was -24% for NO<sub>2</sub> and +47% for NO. In their study, they think the large bias in NO and NO<sub>2</sub> where due to uncertainties in NO<sub>x</sub> emissions and a poor representation of the nocturnal boundary layer by YSU. However, in the above mentioned bias range, results of the MYJ scheme are given as well, and these are still much higher than biases found in our study.

## 5.2 Temporal and spatial patterns

The model captures quite well the daily cycle of NO<sub>2</sub> in the city, which can be described as high values in the morning around 8 am local time (LT), somewhat or much lower concentrations during the day, and a (sometimes less distinct) evening high around 23h LT. The NO cycle can be described as a morning peak around 8 am LT and low concentrations during the rest of the day and during the night. WRF underestimates the morning peak and finds generally too high values in the evening and night for this cycle.

The daily cycle in NO<sub>2</sub> concentration is probably for a large part caused by the development of the mixed layer during daytime: the concentrations are well mixed in the vertical and will become lower on ground level. Morning and evening rush hours probably have amplified the morning peak and the build-up of NO<sub>2</sub> in the afternoon, in particular during winter and early spring, when the emissions take place in a more stable (night-time) boundary layer.

NO has a comparable cycle, but is converted into NO<sub>2</sub> in the late afternoon and particularly after sunset when the NO<sub>2</sub> peak is present, because the backward reaction is not present then. This causes the absence of the evening NO peak.

When maps of the NO or NO<sub>2</sub> concentrations are plotted, the emission sources of NO<sub>x</sub> and the influence of advection become visible. The spatial data on the scale of Amsterdam, however, cannot be validated by satellite data, and the network of point measurements of the GGD is not dense enough to validate the spatial pattern.

In the satellite comparison, the concentrations are specified on a 4x4 km<sup>2</sup> grid for domain 2. This gives higher peaks and lower lows than found for domain 1 (8x8 km<sup>2</sup> grid), which leads to larger differences with satellite data, that are specified on a much larger grid of at least 24x13 km<sup>2</sup> (Boersma et al., 2007).

The satellite observations are not direct observations but columns concentrations based on absorption spectroscopy and a model which determines NO<sub>2</sub> profile shapes and stratospheric background concentrations (Boersma et al., 2007). Evaluations of the previous DOMINO version 1.0 of tropospheric NO<sub>2</sub> retrievals by OMI indicated a general agreement between observations and satellite data, however, biases in the satellite observations of 0-40% were found as well (Boersma et al., 2011). Celarier et al. found that OMI version 1.0 underestimated the tropospheric NO<sub>2</sub> column by 15%-30%, particularly close to NO<sub>2</sub> sources (Celarier et al., 2008). In the improved DOMINO version 2.0, which is used for comparison in this analysis, several factors for retrieving NO<sub>2</sub> are updated: there is a new albedo

database, a new air mass factor is applied, a correction is made in the surface height calculation and the weekly cycle in  $\text{NO}_x$  emissions is corrected (Boersma et al., 2011). So the biases are expected to be lower and it is unlikely that the biases can explain the differences between our model and the OMI satellite concentrations. As DOMINO version 2.0 is a new product, it has not been validated in numerous studies, however, the found bias in DOMINO version 2.0 over different places in Asia was  $-10 \pm 14\%$  (Irie et al., 2012).

Another important remark is that tropospheric column concentrations are based on the whole tropospheric column of 12 km height, but are in practice representing the  $\text{NO}_2$  concentrations over the lowest 1.5 km as the largest part of the  $\text{NO}_2$  molecules does not come higher than 1.5 km (Figure 25). This, however, does still not mean that ground concentrations are represented by the satellite: between July 8 and March 27 and between a city and a rural location, the ground concentrations really differ, but so do the vertical profiles. High ground concentrations are not always found back in the higher atmosphere: on July 8, for example the  $\text{NO}_x$  profile show 5 times as high concentrations on ground level as at 200 meters height over the city (Figure 25). For March 27 the ground-level concentrations are only 2 times as high as 200 meter concentrations over the city (Figure 25). In the rural area, ground concentrations are lower than city ground concentrations, but higher up in the atmosphere higher concentrations are found than at the same height over the city (Figure 25).

In the vertical profile, it is shown that the lowest layers are thus most important in determining the vertical column concentrations. The OMI-satellite, however, is less sensitive near the surface (Folkert Boersma, personal communication), especially in areas with high emission and thus high surface concentrations the model can give biases. This could be part of the reason for mismatch of the Ruhr plume.

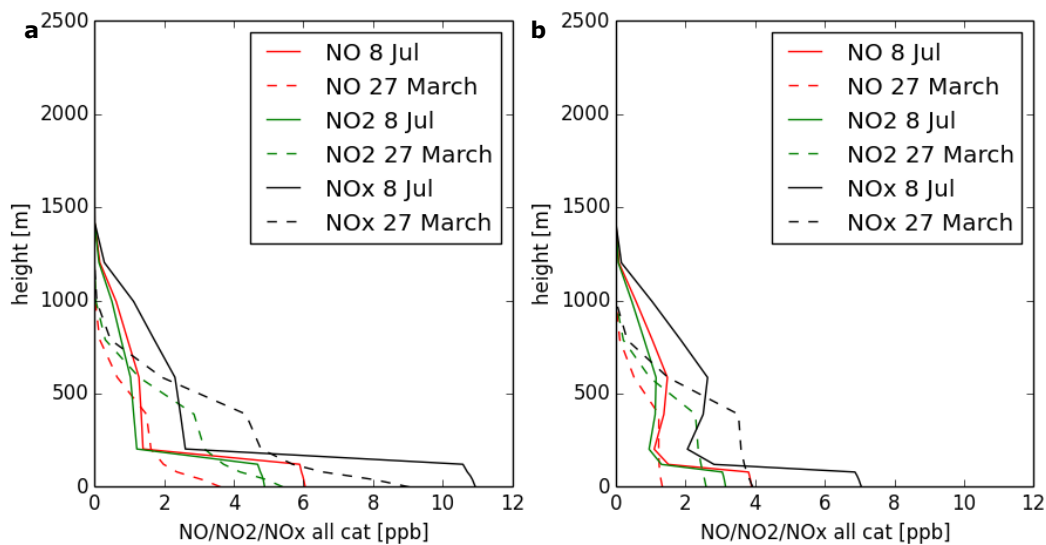


**Figure 25** Vertical distribution  $\text{NO}$ ,  $\text{NO}_2$  and  $\text{NO}_x$  [ppb] 10 am LT for (a) location in Amsterdam and (b) location in the rural area, north-east of Amsterdam

The OMI satellite covers Western Europe only a few times a day and always around 12 am. On this time, however,  $\text{NO}_2$  columns are lowest (Figure 26) as during daytime  $\text{NO}_2$  is converted fastest to  $\text{NO}$ , while during night, the reaction is only the other way around and  $\text{NO}_x$  is present almost exclusively as  $\text{NO}_2$ . When comparing satellite pictures of different times, it is thus important to take the time into account.

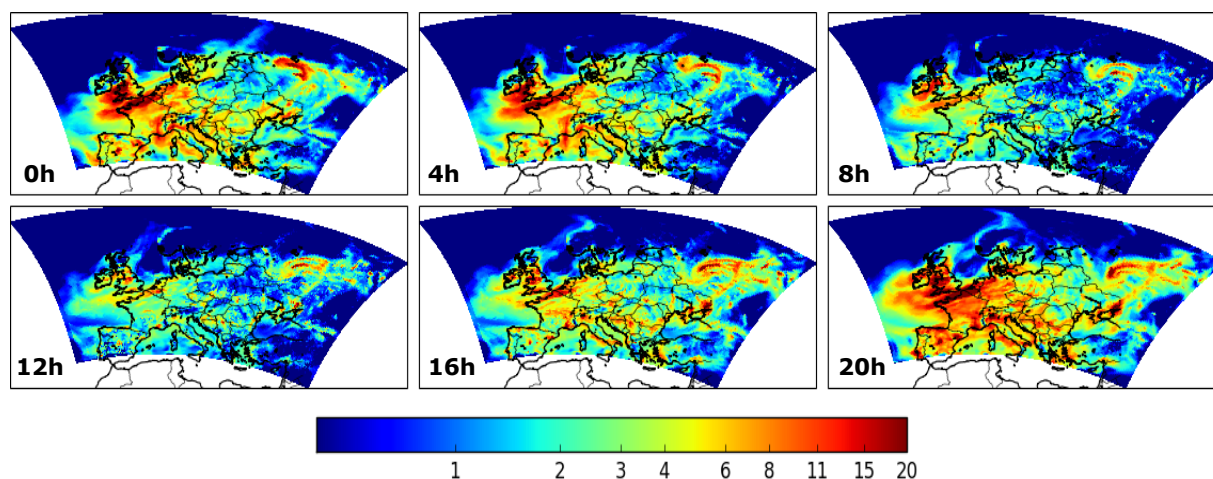


Figure 26 Change in time of tropospheric NO<sub>2</sub> columns [ $10^{15}$  molec/cm<sup>2</sup>] July 8 2013. The times in the lower left are UTC times

### 5.3 Commuters' exposure

As found in our study, the urban background stations in Amsterdam in 2013 had a yearly average NO<sub>2</sub> concentration of 25.9  $\mu\text{g}/\text{m}^3$ . According to a European wide study, yearly average NO<sub>2</sub> concentrations between 2008 and 2011 in the Netherlands and Belgium are 18  $\mu\text{g}/\text{m}^3$  for regional background stations, 28  $\mu\text{g}/\text{m}^3$  for urban background stations and 40  $\mu\text{g}/\text{m}^3$  for traffic stations (Cyrus et al., 2012). The modelled days used in our study have most of the time lower concentrations than the yearly average for urban background stations. For a city in Northern Europe, like Copenhagen (13  $\mu\text{g}/\text{m}^3$  as yearly average urban background concentration), Paris (30  $\mu\text{g}/\text{m}^3$ ) and London (32  $\mu\text{g}/\text{m}^3$ ) urban background NO<sub>2</sub> concentrations were relatively high in the Netherlands, especially when the city size is taken into account (Cyrus et al., 2012). Compared to the excess mortality rate of +5% per 10  $\mu\text{g}/\text{m}^3$  more NO<sub>2</sub> (Hoek et al., 2013), in the Netherlands, mortality is around 7.5% higher in comparison with mortality in Copenhagen and comparable with excess mortality due to air pollution in Paris and London.

For the exposure due to cycling over the chosen routes, in general, the afternoon exposures were found lower than the morning exposures, except for the days in March. The lowest exposures were found in the begin of the afternoon but differ in time for the morning: on March 25 and April 23 was the lowest exposure on 7 am, on July 10 it was 8 am and on July 22 it was 10 am LT.

March 25 was a cold day with very strong easterly winds, on average 5 Beaufort. The sunrise is at about 6:30 LT; boundary layer growth occurs only after 9 am LT. The strong easterly prevents the formation of a stable boundary layer at night; the PBL grows from 550 meters during night to 800 meters at 14h LT. Routes 1a and 1b lay east-west orientated, 1a goes through the city centre, while 1b goes more along the southern border of Amsterdam and closer to the highway. These factors together can explain the exposure pattern of low morning values and high afternoon values. The lowest NO<sub>2</sub> exposure is found very early in the morning, as the rush hour has not been really started yet. The strong easterlies will cause NO<sub>2</sub> advection from the east, causing increasing NO<sub>2</sub> exposure during the day. The somewhat lowered concentrations at 10h and 16h are probably caused by the late, limited growth of the boundary layer. The higher exposure found on route 1b, compared to route 1a on March 25 is probably caused by the easterly: east of route 1b the concentrations are higher than east of route 1a, which gets more of the relative fresh air of the lake IJmeer (see also Figure 11). The fact that routes 2a and 2b have a quite similar exposure, is probably a result of the fact that concentrations are more dependent on advection with the high wind speeds and of the balance between the extra emissions that are in between route 2b and 2a with an easterly, and the fact that route 2b is 2 km longer.

The wind turns between southwest and west and has a speed of 3 bft on April 23. The exposure difference between 2a and 2b on April 23 is somewhat higher than what could be caused by the length difference, this is probably caused by the emissions in between 2a and 2b. As 1a and 1b are parallel to

the wind direction and emission sources are not very different to the West of Amsterdam, the exposures are the same for this routes.

July 10 and July 22 are summer days, which explains the already low values at 8 am departure: the mixed layer growth starts earlier in the morning and is already well developed at 8 am, while the emissions have not been very high. The highest afternoon exposures are found on the time where the mixed layer is collapsing, while the emissions of daytime and afternoon rush hour have been built up. The north wind of July 10 can be a good explanation of the higher exposure on route 1a: it lays north of route 1b and will thus get less city emissions. As part of the routes 2a and 2b are east-west orientated as well, the north wind can explain the difference between these routes as well. On July 22 the wind speeds are low and the direction is variable, which explains the differences between 1a and 1b as well as between 2a and 2b are close to the differences between the lengths of the respective routes. The higher mixed layer on July 22 outbalances the high emissions in the morning rush-hour: due to the mixing the concentrations do not increase in the morning.

**Table 13 Average measured NO<sub>2</sub> concentrations for the rush-hours on the four stations: Vondelpark, Sportpark Ookmeer, Oude Schans and Stadhouderskade, underestimations by the model and factor between measured and modelled values.**

	Average measured rush hour NO <sub>2</sub> concentration [µg/m <sup>3</sup> ]	Rush hour average over/underestimation [µg/m <sup>3</sup> ]	Factor measured over modelled
<b>March 25</b>	18.1	-12.9	3.4
<b>April 23</b>	28.9	-1.6	1.1
<b>July 10</b>	18.9	-8.8	1.9
<b>July 22</b>	36.7	-6.0	1.2

**Table 14 Average NO<sub>2</sub> concentrations [µg/m<sup>3</sup>] along route 1a and 2a on 8 am LT , model output and estimated according to the factors between modelled and measured concentration which could be found back in Table 13**

route	Modelled along-route average concentration [µg/m <sup>3</sup> ]				Estimated along-route average concentration [µg/m <sup>3</sup> ]			
	March 25	April 23	July 10	July 22	March 25	April 23	July 10	July 22
<b>1</b>	5.4	40.4	12.0	41.4	18.2	42.9	22.4	49.3
<b>2</b>	6.8	37.0	12.4	42.5	23.0	39.2	23.2	50.6

Especially on days with high NO<sub>2</sub> concentrations as April 23 and July 22 the differences in exposure will be important in determining long-term health effects. Each increase in NO<sub>2</sub> and thus increase in pollutant concentration will lead to a higher chance on health problems, but as the absolute differences are larger, relative differences will be more significant. On March 25 the measured NO<sub>2</sub> concentration was on average 16.51 µg/m<sup>3</sup> for the four stations Vondelpark, Sportpark Ookmeer, Oude Schans Centrum and Stadhouderskade, for 23 April this was 28.38 µg/m<sup>3</sup>, for 10 July 15.72 µg/m<sup>3</sup> and for 22 July 31.69 µg/m<sup>3</sup> (Table 13). The average NO<sub>2</sub> concentrations along the routes on 8 am LT have been calculated as well (Table 14). What could be seen, is that on April 23 and July 22, the estimated concentrations are above the WHO guidelines of 40 µg/m<sup>3</sup>. The guidelines of 40 µg/m<sup>3</sup> are however for yearly averaged values, and in this study these are only 8 o'clock rush-hour concentrations which are close to the maximum concentrations and do not represent the inhaled concentrations the remainder of the day.

We found minimal influence of cycling the route the other way around, thus in the morning from the endpoint to the start point and in the evening from start to end. The exposure found was between 92% and 104% of the exposures on the route in the normal direction.

The exposure found in this study is now based on the concentration values WRF gave for the different grid cells which were part of the routes. The correlation between WRF and measurement is reasonable but WRF is not matching the observations perfectly. This makes it possible that the patterns in real do deviate from the shown patterns. Besides, it is important to remember that the concentrations found by WRF are better representative for background stations than for high traffic roads. Emissions inhaled as a result of a moped driving in front of a commuter for some length or waiting for a traffic light, while

stationary traffic keeps emitting near the commuter will outbalance the background city concentrations used for making up the balance.

Nonetheless, this study gives a good overview of the exposure based on the background concentrations and thus of the amount of pollutants which is inhaled at least. In the choice of route this is most important, as the driving along of a moped, old diesel car or heavy truck is much less predictable and could thus occur on any route. The results show large advantages of making a smart choice in route, as the differences between different times of leaving and different routes are substantial. While the WHO and European Union made limits on concentrations of pollutants in the air, any increase in inhaled concentrations of pollutants will lead to a higher risks on diseases as COPD, cardiac-diseases and cancer and increases the excess mortality rate and should thus be prevented.

## 6. Conclusions

Moderate to strong correlations between model results and NO and NO<sub>2</sub> observations were found, especially for city background stations. Performance of the model is found weak at days with more extreme weather conditions (i.e. cold and hot days).

Temperatures were slightly underestimated by WRF for the city of Amsterdam, the underestimation however, probably hardly influences the found NO and NO<sub>2</sub> concentrations.

Two days were suitable for satellite comparison. The day in July gave comparable results: general patterns were the same between model and satellite, on average there was a small underestimation found in the model. For the day in March less similarities were found, the modelled NO<sub>2</sub> concentrations were found much lower, this could have been partly due to a too slow NO to NO<sub>2</sub> conversion.

For the urban background stations in Amsterdam a yearly average NO<sub>2</sub> concentration of 25.9 µg/m<sup>3</sup> was found for 2013. The average concentration over 2013 for traffic station Stadhouderskade was 39.8 µg/m<sup>3</sup>.

The results of the present study show a large spatial and temporal variability of NO<sub>x</sub> concentrations in Amsterdam. The chosen route to the city centre and the departure time are important for determining the exposure value. Differences of more than 100% were found between different times of cycling.

The weather influenced the departure time with lowest exposure. On days with a large boundary layer development, concentrations are already mixed some time after sunset and later in the morning lower exposure is found. On other days, the lowest concentrations are found before the start of the rush hour. The afternoon values are generally lower than the morning values and increased with time as the mixed layer collapsed. Only on days with limited boundary layer growth, the afternoon values are higher polluted.

The wind direction influences the cleanest cycle route, higher exposure have been found with winds coming from upwind sources like the city centre or the south-east of Amsterdam.

## 7. Recommendations

To make the model more constant in giving reliable results, a couple of things could be tried for improvement:

- More species could be added for chemistry: VOCs, OH, etc.
  - This makes it possible as well to use other chemistry functions of WRF-chem.
  - This will lead as well to more realistic ozone concentrations, which will improve the reaction speed of Reaction 1
- Use could be made of 1x1 km<sup>2</sup> or finer resolution emission for all emission categories over Amsterdam. This will improve the spatial pattern of NO<sub>2</sub> on city scale.
- If it is structural (on some places) that concentrations in WRF deviate from the concentrations found by satellite, the emission pattern could be adapted from satellite observations

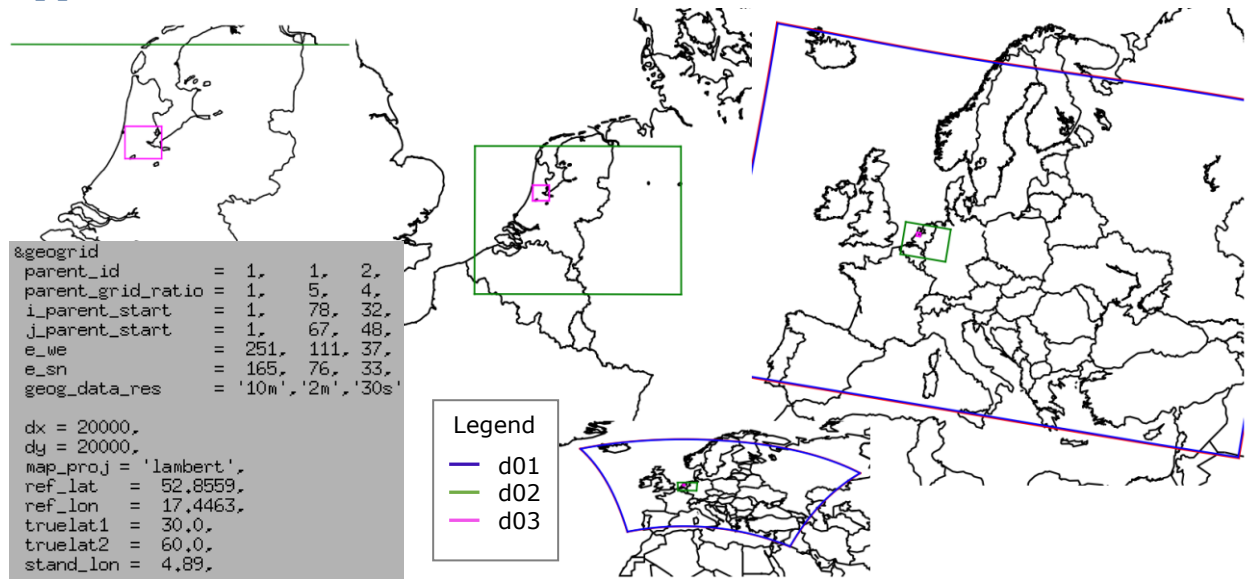
## References

- ANP, Weer 80 rijden op A10 en A13. *AD* (2014).
- Arnfield, A.J., Two decades of urban climate research: a review of turbulence, exchanges of energy and water, and the urban heat island, *Int J Climatol* **23**(2003), pp. 1-26.
- Beelen, R., Hoek, G., van den Brandt, P.A., Goldbohm, R.A., Fischer, P., Schouten, L.J., Jerrett, M., Hughes, E., Armstrong, B. and Brunekreef, B., Long-term effects of traffic-related air pollution on mortality in a Dutch cohort (NLCS-AIR study), *Environmental Health Perspectives* **116**(2008), p. 196.
- Berkowicz, R., OSPM - A parameterised street pollution model, *Environ Monit Assess* **65**(2000a), pp. 323-331.
- Berkowicz, R., A simple model for urban background pollution, *Environ Monit Assess* **65**(2000b), pp. 259-267.
- Bernstein, J.A., Alexis, N., Barnes, C., Bernstein, I.L., Nel, A., Peden, D., Diaz-Sanchez, D., Tarlo, S.M. and Williams, P.B., Health effects of air pollution, *Journal of Allergy and Clinical Immunology* **114**(2004), pp. 1116-1123.
- Boersma, K., Eskes, H., Veefkind, J.P., Brinksma, E., Sneep, M., Van den Oord, G., Levelt, P., Stammes, P., Gleason, J. and Bucsele, E., Near-real time retrieval of tropospheric NO<sub>2</sub> from OMI, *Atmospheric Chemistry & Physics* **7**(2007).
- Boersma, K.F., Eskes, H.J., Dirksen, R.J., van der A, R.J., Veefkind, J.P., Stammes, P., Huijnen, V., Kleipool, Q.L., Sneep, M., Claas, J., Leitão, J., Richter, A., Zhou, Y. and Brunner, D., An improved tropospheric NO<sub>2</sub> column retrieval algorithm for the Ozone Monitoring Instrument, *Atmos. Meas. Tech.* **4**(2011), pp. 1905-1928.
- Case, J.L., Crosson, W.L., Kumar, S.V., Lapenta, W.M. and Peters-Lidard, C.D., Impacts of High-Resolution Land Surface Initialization on Regional Sensible Weather Forecasts from the WRF Model, *Journal of Hydrometeorology* **9**(2008).
- CBS, Bevolkingsontwikkeling; regio per maand. In: C.B.v.d. Statistiek, Editor, *StatLine*, CBS (2013).
- Celarier, E., Brinksma, E., Gleason, J., Veefkind, J., Cede, A., Herman, J., Ionov, D., Goutail, F., Pommereau, J.P. and Lambert, J.C., Validation of Ozone Monitoring Instrument nitrogen dioxide columns, *Journal of Geophysical Research: Atmospheres* (1984-2012) **113**(2008).
- Chan, C.K. and Yao, X., Air pollution in mega cities in China, *Atmos Environ* **42**(2008), pp. 1-42.
- Cheng, W.Y. and Steenburgh, W.J., Evaluation of surface sensible weather forecasts by the WRF and the Eta models over the western United States, *Weather & Forecasting* **20**(2005).
- Collins, W., Stevenson, D.S., Johnson, C. and Derwent, R., Tropospheric ozone in a global-scale three-dimensional Lagrangian model and its response to NO<sub>x</sub> emission controls, *Journal of Atmospheric Chemistry* **26**(1997), pp. 223-274.
- Coniglio, M.C., Correia, J., Marsh, P.T. and Kong, F.Y., Verification of Convection-Allowing WRF Model Forecasts of the Planetary Boundary Layer Using Sounding Observations, *Weather Forecast* **28**(2013), pp. 842-862.
- Cyrys, J., Eeftens, M., Heinrich, J., Ampe, C., Armengaud, A., Beelen, R., Bellander, T., Beregszaszi, T., Birk, M., Cesaroni, G. et al., Variation of NO<sub>2</sub> and NO<sub>x</sub> concentrations between and within 36 European study areas: Results from the ESCAPE study, *Atmos Environ* **62**(2012), pp. 374-390.
- Deira, S., Schultz moet snelheidsverhoging A10 opnieuw bekijken. *Elsevier*, ANP (2014).
- Den Boeft, J., Eerens, H.C., Den Tonkelaar, W. and Zandveld, P., CAR International: A simple model to determine city street air quality, *Science of the total environment* **189**(1996), pp. 321-326.
- DIVV, Fietsen in Amsterdam - Factsheet meerjarenplan fiets. (2012a).
- DIVV, Meerjarenplan Fiets 2012-2016. In: D.D.I.V.e.V.G. Amsterdam, Editor, Amsterdam (2012b), pp. 1-64.
- Doorn, P.K. and Rhebergen, M.P., Statistiek voor Historico. *Correlation and Regression*, University of Leiden, Leiden (2006).
- Düring, I., Bächlin, W., Ketzler, M., Baum, A., Friedrich, U. and Wurzler, S., A new simplified NO/NO<sub>2</sub> conversion model under consideration of direct NO<sub>2</sub>-emissions, *Meteorologische Zeitschrift* **20**(2011), pp. 67-73.
- EC, Air Quality Standards. European Commission. In: E. Commission, Editor, *Environment* (2013).
- Ek, M.B., Mitchell, K.E., Lin, Y., Rogers, E., Grunmann, P., Koren, V., Gayno, G. and Tarpley, J.D., Implementation of Noah land surface model advances in the National Centers for Environmental Prediction operational mesoscale Eta model, *J. Geophys. Res.* **108**(2003), p. 8851.
- Elshazly, S., Takahashi, M., Adam, M.E.-N. and Hassan, A., Simulation of Some Air Pollutants and Weather Parameters Using WRF/Chem Model in Cairo and Qena Cities/Egypt, *World Environment* **2**(2012), pp. 127-134.
- Fast, J.D., Gustafson, W.I., Easter, R.C., Zaveri, R.A., Barnard, J.C., Chapman, E.G., Grell, G.A. and Peckham, S.E., Evolution of ozone, particulates, and aerosol direct radiative forcing in the vicinity of Houston using a fully coupled meteorology-chemistry-aerosol model, *Journal of Geophysical Research: Atmospheres* (1984-2012) **111**(2006).
- Fietsberaad, Amsterdam telt 881.000 fietsen. (2012).
- Fowler, D., Amann, M., Anderson, R., Ashmore, M., Cox, P., Depledge, M., Derwent, D., Grennfelt, P., Hewitt, N., Hov, O., Jenkin, M., Kelly, F., Liss, P., Pilling, M., Pyle, J., Slingo, J., Stevenson, D., Fowler, D., Amann, M., Anderson, R., Ashmore, M., Cox, P., Depledge, M., Derwent, D., Grennfelt, P., Hewitt, N., Hov, O., Jenkin, M., Kelly, F., Liss, P., Pilling, M., Pyle, J., Slingo, J. and Stevenson, D., *Ground-level ozone in the 21st century: future trends, impacts and policy implications*, The Royal Society, London (2008).
- GGD, Luchtverontreiniging Amsterdam 2012. In: C.I.a. luchtkwaliteit, Editor, Amsterdam (2012).
- Grell, G.A., Peckham, S.E., Schmitz, R., McKeen, S.A., Frost, G., Skamarock, W.C. and Eder, B., Fully coupled "online" chemistry within the WRF model, *Atmos Environ* **39**(2005), pp. 6957-6975.
- Heijne, S., Lucht in grote steden is nog zeer ongezond. *Volkskrant* (2013).

- Hoek, G., Krishnan, R.M., Beelen, R., Peters, A., Ostro, B., Brunekreef, B. and Kaufman, J.D., Long-term air pollution exposure and cardio-respiratory mortality: a review, *Environ Health* **12**(2013), p. 43.
- Irie, H., Boersma, K., Kanaya, Y., Takashima, H., Pan, X. and Wang, Z., Quantitative bias estimates for tropospheric NO<sub>2</sub> columns retrieved from SCIAMACHY, OMI, and GOME-2 using a common standard for East Asia, *Atmos Meas Tech* **5**(2012), pp. 2403-2411.
- Jacob, D.J., *Introduction to atmospheric chemistry*, Princeton University Press, Princeton, NJ (1999) XII, 266 p pp.
- Jacob, D.J. and Winner, D.A., Effect of climate change on air quality, *Atmos Environ* **43**(2009), pp. 51-63.
- Janjić, Z.I., Nonsingular implementation of the Mellor–Yamada level 2.5 scheme in the NCEP Meso model, *NCEP office note* **437**(2002), p. 61.
- Kakosimos, K.E., Hertel, O., Ketznel, M. and Berkowicz, R., Operational Street Pollution Model (OSPM)–a review of performed application and validation studies, and future prospects, *Environmental Chemistry* **7**(2010), pp. 485-503.
- Knol, A., Stumpe, I., Hoe gezond is onze lucht? Halfjaar rapportage meetcampagne oktober 2012 - juli 2013. In: Milieudefensie, Editor, Milieudefensie, Amsterdam (2013).
- Kuenen, J., van der Gon, H.D., Visschedijk, A., van der Brugh, H. and van Gijlswijk, R., MACC European emission inventory for the years 2003–2007, *TNO-report TNO-060-UT-2011-00588*, Utrecht(2011).
- Legates, D.R. and McCabe, G.J., Evaluating the use of “goodness-of-fit” measures in hydrologic and hydroclimatic model validation, *Water resources research* **35**(1999), pp. 233-241.
- Minoura, H., Some characteristics of surface ozone concentration observed in an urban atmosphere, *Atmospheric research* **51**(1999), pp. 153-169.
- Misenis, C. and Zhang, Y., An examination of sensitivity of WRF/Chem predictions to physical parameterizations, horizontal grid spacing, and nesting options, *Atmospheric research* **97**(2010), pp. 315-334.
- Mönkkönen, P., Koponen, I., Lehtinen, K., Hämeri, K., Uma, R. and Kulmala, M., Measurements in a highly polluted Asian mega city: observations of aerosol number size distribution, modal parameters and nucleation events, *Atmospheric Chemistry and Physics* **5**(2005), pp. 57-66.
- Morree, J.J.d., Jongert, T. and Poel, G.M., *Inspanningsfysiologie, oefentherapie en training*, Bohn Stafleu van Loghum (2011).
- Nguyen, L. and Wesseling, J., OSPM: Comparison between modelled results obtained for the Erzeijstraat in the Netherlands and measurements, *RIVM report* **680705011**(2009).
- Ouwensloot, H.G., The impact of dynamic processes on chemistry in atmospheric boundary layers over tropical and boreal forest. Wageningen University, Wageningen (2013), p. 208 p.
- Pope III, C.A. and Dockery, D.W., Health effects of fine particulate air pollution: lines that connect, *Journal of the Air & Waste Management Association* **56**(2006), pp. 709-742.
- RIVM, Trends in PM<sub>10</sub>- en NO<sub>2</sub>-concentraties in Nederland tot en met 2010 - Gezamenlijke trendanalyse van RIVM, DCMR, GGD Amsterdam. In: R.v.V.e. Milieu, Editor (2012).
- RIVM, Achtergrond document NO<sub>2</sub> (RIVM). In: RIVM, Editor (2013a).
- RIVM, Concentraties in 2012: PM10 en NO2 lager dan in voorgaande jaren. In: R.v.V.e. Milieu, Editor (2013b).
- RIVM, Kans op matige ozonmog op maandag 22 juli en dinsdag 23 juli. (2013c).
- Schultz, M., Backman, L., Balkanski, Y., Bjoerndalsaeter, S., Brand, R., Burrows, J., Dalsoeren, S., de Vasconcelos, M., Grodtmann, B. and Hauglustaine, D., REanalysis of the TROpospheric chemical composition over the past 40 years (RETRO)–A long-term global modeling study of tropospheric chemistry, *Final Report, Jülich/Hamburg, Germany* **2007**(2007).
- Seinfeld, J.H. and Pandis, S.N., *Atmospheric chemistry and physics: from air pollution to climate change*, John Wiley & Sons (1998).
- Service/NOAA/U.S. N.C.f.E.P.N.W., NCEP FNL Operational Model Global Tropospheric Analyses, continuing from July 1999. In: C.a.I.S.L. Research Data Archive at the National Center for Atmospheric Research, Editor, Department of Commerce (2000, updated daily).
- Skamarock, W.C., Klemp, J.B., Dudhia, J., Gill, D.O., Barker, D.M., Duda, M.G., Huang, X.-Y., Wang, W. and Powers, J.G., A Description of the Advanced Research WRF Version 3. *NCAR Technical Note*, Mesoscale and Microscale Meteorology Division - National Center for Atmospheric Research, Boulder, Colorado, USA (2008), pp. 1-125.
- Stensrud, D.J., *Parameterization schemes: keys to understanding numerical weather prediction models*, Cambridge University Press (2007).
- Tie, X., Brasseur, G. and Ying, Z., Impact of model resolution on chemical ozone formation in Mexico City: application of the WRF-Chem model, *Atmospheric Chemistry and Physics* **10**(2010), pp. 8983-8995.
- Trebs, I., Bohn, B., Ammann, C., Rummel, U., Blumthaler, M., Königstedt, R., Meixner, F.X., Fan, S. and Andreae, M.O., Relationship between the NO<sub>2</sub> photolysis frequency and the solar global irradiance, *Atmos Meas Tech* **2**(2009), pp. 725-739.
- van der Gon, H.D., Hendriks, C., Kuenen, J., Segers, A. and Visschedijk, A., Description of current temporal emission patterns and sensitivity of predicted AQ for temporal emission patterns. TNO (2011).
- WHO, Air quality and health. In: WHO, Editor, *Media centre - fact sheet* (2011).
- Willems, M., De twintig meest vervuilde plekken in Nederland volgens Milieudefensie. *NRC*, NRC, Rotterdam (2013).
- Willmott, C.J., Some comments on the evaluation of model performance, *Bulletin of the American Meteorological Society* **63**(1982), pp. 1309-1313.
- Yao, X., Lau, N., Chan, C. and Fang, M., The use of tunnel concentration profile data to determine the ratio of NO<sub>2</sub>/NO<sub>x</sub> directly emitted from vehicles, *Atmospheric Chemistry and Physics Discussions* **5**(2005), pp. 12723-12740.

- Zhang, Y., Dubey, M.K., Olsen, S.C., Zheng, J. and Zhang, R., Comparisons of WRF/Chem simulations in Mexico City with ground-based RAMA measurements during the 2006-MILAGRO, *Atmos. Chem. Phys.* **9**(2009), pp. 3777-3798.
- Zuurbier, M., Hoek, G., van den Hazel, P. and Brunekreef, B., Minute ventilation of cyclists, car and bus passengers: an experimental study, *Environ Health* **8**(2009).

## Appendix



Appendix Figure I Description and depicting of model (nested) domains.

Appendix Table I Number of observations used for calculation of Correlation Coefficients and  $R^2$  on whole days (24 hour), days (7am LT till 6 pm LT) and nights (7 pm LT till 6 am LT)

	N whole day				N day				N night			
	Von	OS	StdK	Ook	Von	OS	StdK	Ook	Von	OS	StdK	Ook
<b>25 March</b>	21	23	23	23	10	12	12	12	11	11	11	11
<b>26 March</b>	24	24	22	24	12	12	10	12	12	12	12	12
<b>27 March</b>	22	24	24	24	10	12	12	12	12	12	12	12
<b>19 April</b>	22	22	22	23	12	12	12	12	10	10	10	11
<b>20 April</b>	22	24	23	24	12	12	12	12	10	12	11	12
<b>21 April</b>	24	24	23	24	12	12	12	12	12	12	11	12
<b>22 April</b>	22	23	22	23	12	12	12	12	10	11	10	11
<b>23 April</b>	23	24	24	24	12	12	12	12	11	12	12	12
<b>24 April</b>	24	24	22	24	12	12	12	12	12	12	10	12
<b>6 July</b>	23	23	21	23	12	12	10	12	11	11	11	11
<b>7 July</b>	22	24	24	24	10	12	12	12	12	12	12	12
<b>8 July</b>	24	24	22	24	12	12	10	12	12	12	12	12
<b>10 July</b>	23	23	21	23	12	12	10	12	11	11	11	11
<b>11 July</b>	22	13	24	24	10	8	12	12	12	5	12	12
<b>12 July</b>	24	0	22	24	12	0	10	12	12	0	12	12
<b>21 July</b>	21	23	23	23	12	12	12	12	9	11	11	11
<b>22 July</b>	24	24	22	24	12	12	12	12	12	12	10	12
<b>23 July</b>	22	23	23	24	12	11	11	12	10	12	12	12

Appendix Table II Correlation Coefficients of NO<sub>2</sub> split to day and night: day = 7-18 LT, night = 19-6 LT. Acronyms: Von = Vondelpark, OS=Oude Schans Centrum, StdK=Stadhouderskade, Ook=Sportpark Ookmeer. The number of measurements (N) per day/night and station can be found

Date (2013)	Correlation Coefficient NO <sub>2</sub>							
	Von day	Von night	OS day	OS night	StdK day	StdK night	Ook day	Ook night
25 March <sup>1</sup>	0.54	0.82	0.33	0.96	0.49	0.88	0.83	0.90
26 March	0.49	0.89	0.53	0.90	0.22	0.93	0.38	0.67
27 March	0.22	0.92	0.68	0.97	0.27	0.93	0.44	0.88
19 April <sup>1</sup>	-0.04	-0.34	-0.30	-0.29	0.63	-0.24	0.29	-0.40
20 April	0.48	-0.81	0.67	-0.49	0.27	-0.46	0.94	-0.56
21 April	0.35	0.01	-0.37	0.63	0.11	0.81	0.33	0.59
22 April <sup>1</sup>	0.69	-0.12	0.56	0.27	0.37	0.61	0.80	0.52
23 April	0.86	0.83	0.90	0.86	0.87	0.74	0.91	0.77
24 April	0.93	0.51	0.91	0.79	0.80	-0.35	0.98	0.66
6 July <sup>1</sup>	0.80	0.93	-0.25	0.68	-0.68	0.65	0.76	0.86
7 July	0.88	0.78	-0.47	0.19	-0.67	-0.88	0.89	-0.24
8 July	0.85	0.23	-0.68	-0.40	0.14	-0.80	0.63	0.26
10 July <sup>1</sup>	0.86	0.56	0.60	0.44	0.13	0.47	0.70	0.70
11 July <sup>2</sup>	0.06	0.71	-0.56	-0.10	0.47	0.70	-0.11	-0.80
12 July <sup>2</sup>	0.36	0.44			0.44	0.54	0.78	0.52
21 July <sup>1</sup>	0.49	0.62	-0.55	0.85	-0.59	0.72	0.89	0.83
22 July	0.83	0.73	0.91	0.12	-0.01	-0.72	0.81	-0.16
23 July	0.56	-0.66	0.92	-0.16	0.06	-0.79	0.76	-0.61
<b>average</b>	<b>0.57</b>	<b>0.39</b>	<b>0.23</b>	<b>0.37</b>	<b>0.19</b>	<b>0.21</b>	<b>0.67</b>	<b>0.30</b>
week	<b>0.55</b>	<b>0.43</b>	<b>0.40</b>	<b>0.36</b>	<b>0.38</b>	<b>0.22</b>	<b>0.63</b>	<b>0.30</b>
weekend	<b>0.60</b>	<b>0.31</b>	<b>-0.19</b>	<b>0.37</b>	<b>-0.31</b>	<b>0.17</b>	<b>0.76</b>	<b>0.30</b>

<sup>1</sup>Data of 00h UTC was excluded from the comparison this day, on these times WRF was still on its initial conditions

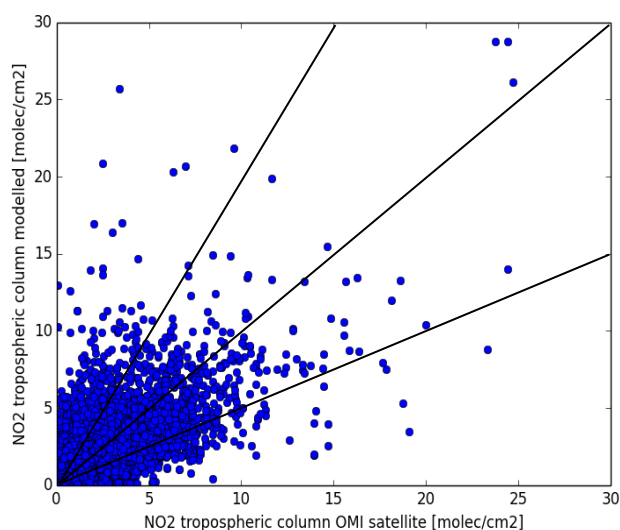
<sup>2</sup>The Oude Schans measurements lack for this day

Appendix Table III Correlation Coefficient for NO<sub>2</sub> over all stations together for 24 hours and for only daytime (7 am LT – 6 pm LT) and only night time (7 pm LT – 6 am LT). The amount of observations (N) is the sum of Von, OS, StdK and Ook of Table 15 in this appendix

Date (2013)	Correlation Coefficient NO <sub>2</sub>		
Correlation coefficient	City stations all	day city stations	night city stations
25 March <sup>1</sup>	0.50	0.20	0.77
26 March	0.50	0.27	0.79
27 March	0.57	0.16	0.86
19 April <sup>1</sup>	0.37	0.39	0.13
20 April	-0.07	0.27	-0.55
21 April	0.20	0.15	0.39
22 April <sup>1</sup>	0.34	0.62	0.45
23 April	0.59	0.64	0.76
24 April	0.60	0.76	0.47
6 July <sup>1</sup>	0.36	0.00	0.60
7 July	-0.15	0.05	-0.24
8 July	-0.13	0.23	-0.15
10 July <sup>1</sup>	0.44	0.49	0.53
11 July <sup>2</sup>	0.22	0.10	0.30
12 July <sup>2</sup>	0.16	0.27	0.32
21 July <sup>1</sup>	0.29	-0.16	0.46
22 July	0.11	0.49	-0.03
23 July	-0.06	0.29	-0.54
<b>average</b>	<b>0.27</b>	<b>0.29</b>	<b>0.30</b>
<b>week</b>	<b>0.32</b>	<b>0.38</b>	<b>0.36</b>
<b>weekend</b>	<b>0.13</b>	<b>0.06</b>	<b>0.13</b>

<sup>1</sup>Data of 00h UTC was excluded from the comparison this day, on these times WRF was still on its initial conditions

<sup>2</sup>The Oude Schans measurements lack for this day



Appendix Figure II Modelled tropospheric NO<sub>2</sub> columns versus OMI satellite observations of the columns [molec/cm<sup>2</sup>] include are a 1:1 line, a ½:1 line and a 2:1 line.